Structure of the intermediates in the industrial separation of perinone isomers

Structure of the intermediates in the industrial separation of perinone isomers

Lukas Tapmeyer[a], Michael Bolte[a], Michele R. Chierotti[b], Martin U. Schmidt[a]*
[a]Institute of Inorganic and Analytical Chemistry, Goethe University Frankfurt am Main, Max-von-Laue-Str. 7, 60438 Frankfurt am Main, Germany.
[b]Departement of Chemistry and NIS Centre, University of Torino, V. Giuria 7, 10125 Torino, Italy.
* Corresponding author.
E-mail address: m.schmidt@chemie.uni-frankfurt.de

Abstract

The industrial synthesis of perinone results in a mixed crystal containing an isomer mixture of *trans*- and *cis*-perinone. The isomers are separated by treatment with alcoholic KOH, which leads to a pale yellow precipitate and a yellow solution. The precipitate is subsequently hydrolyzed to produce pure *trans*-perinone (Pigment Orange 43). The yellow solution is treated with dilute acids to give *cis*-perinone (Pigment Red 194). The chemical structure and the stoichiometry of the intermediate pale yellow precipitate has never been determined, although this intermediate has been produced on a multi-ton scale for more than 85 years. The intermediate was assumed to be a "potassium hydroxide addition compound". X-ray single-crystal analyses reveal that this assumption is wrong. The KOH/ethanol treatment actually causes a double ring-opening of the perinone. This results in the tetra-potassium salt of 4,8-bis(benzimidazolato)-naphthalene-1,5-dicarboxylate. Two phases were isolated: The α-phase, $K_4[C_{26}H_{12}N_4O_4] \cdot 3C_2H_5OH \cdot 6H_2O$, from the industrial synthesis and the β-phase, $1.5(K_4[C_{26}H_{12}N_4O_4]) \cdot 5C_2H_5OH \cdot 4H_2O$, from a recrystallization in KOH/ethanol. The molecular and crystal structures are confirmed by solid-state NMR spectroscopy through combination of ^{13}C CPMAS and MAS experiments, which revealed that the solvent layers in the crystals show a highly dynamic solvent disorder in the solid state. The intermediate of *cis*-perinone, which is formed in the isomer separation step, has been isolated as well. Also this intermediate has a ringopened molecular structure, as revealed by single-crystal X-ray diffraction.

1. Introduction

In the chemical industry, there are astonishingly many compounds which are produced on a multi-ton scale for decades, but their molecular structure and chemical composition are still unknown. Two of these compounds are the intermediates in the industrial separation of the perinone isomers in the production of Pigment Orange 43 (*trans*Perinone, P.O.43, **1**, see figure 1).

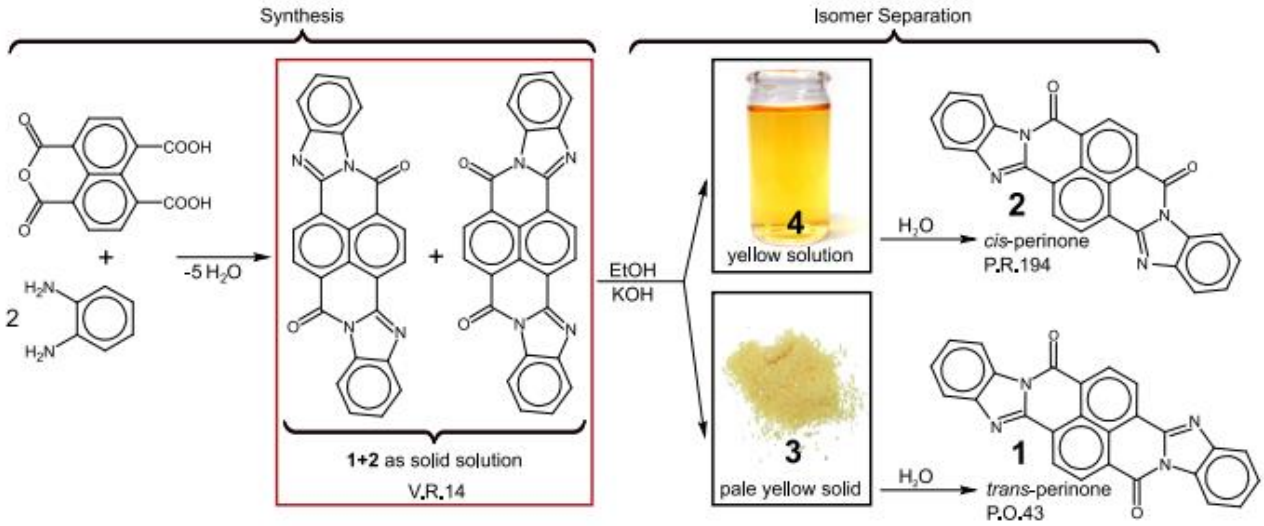

Figure 1: Industrial synthesis and isomer separation of *trans*-perinone (Pigment Orange 43, **1**) and *cis*-perinone (Pigment Red 194, **2**). The structures of the intermediates **3** and **4** are investigated here.

Perinone has been industrially produced for at least 80 years [1]. The industrial synthesis starts from naphthalene-tetracarboxylic mono-anhydride, which is condensed with two equivalents of 1,2-diaminobenzene, see figure 1 left [2,3]. The reaction yields a mixed crystal (solid solution) [2,2] of two isomers, *trans*-perinone (**1**) and *cis*-perinone (**2**) in a ratio of nearly one to one. The mixed crystal is registered as Vat Red 14 (see figure 1 and figure 2). The two isomers are industrially separated by treatment with hot KOH/ethanol (see figure 1); cooling or dilution causes the precipitation of a pale yellow intermediate (**3**), which is isolated by filtration. Astonishingly, the molecular structure and the chemical composition of this intermediate are still unknown. The yellow filtrate contains the other isomers intermediate (**4**) whose structure is unknown as well.

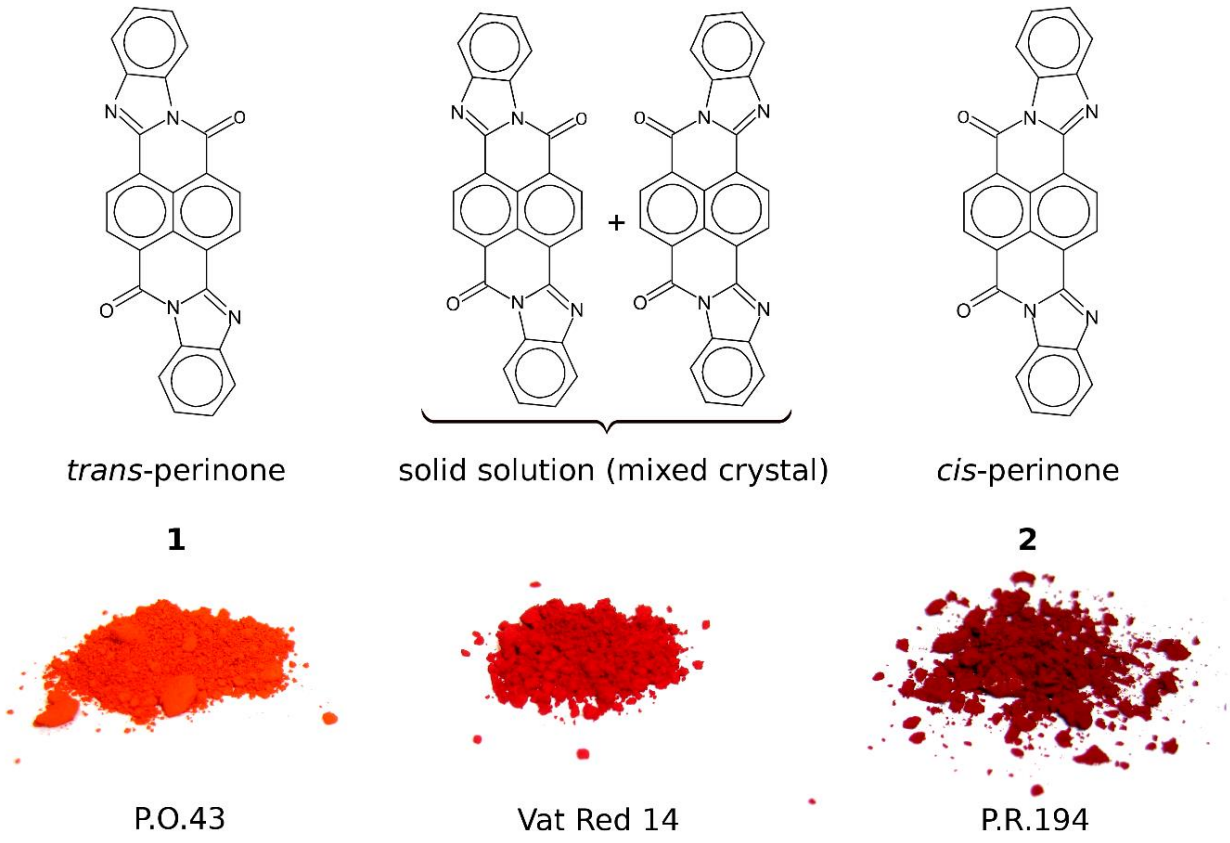

Figure 2: Simplified chemical structures of the perinone isomers and depiction of their colours.

The precipitated intermediate (**3**) is subsequently treated with water, to give the pure *trans*-perinone, Pigment Orange 43 (P.O.43, **1**). The yellow filtrate is treated with diluted acids, resulting in the formation of the red *cis*-perinone, Pigment Red 194 (P.R.194, **2**). [1] Industrially, the intermediate (**4**) is handled only in solution. Nevertheless, this compound (**4**) can be precipitated from a hot, concentrated solution by cooling.
The molecular formulae of *cis*-perinone and *trans*-perinone are known since long. [4,5] Also the crystal structures of *cis*- and *trans*-perinone, as well as of the mixed crystal are known. [2,6–11]
In contrast, the chemical composition or even the molecular structure of the intermediate **3** have apparently never been elucidated, despite of it having been synthesized on a multiton scale for more than 80 years. [4] Also the isolation of **4** as a solid and its chemical structure has apparently never been reported.
In the literature, the intermediate **3** is denominated as "potassium hydroxide addition product"[4,12]. The hitherto assumed molecular formula is shown in figure 4. However, it remains obscure which analytical methods were employed to establish this formula.

Here the intermediate **3** was investigated by single crystal X-ray diffraction, amended by powder X-ray diffraction (PXRD), solution and solid-state NMR and IR spectroscopy. Thereby, the molecular structure, the chemical composition and the crystal structure of **3** have finally been determined. Additionally, the intermediate **4** has been isolated. Its molecular structure and crystal structure have been determined as well.

The perinone isomers can also be separated by two other processes: (a) dissolution of the isomer mixture in concentrated sulfuric acid and fractionated crystallization of the *trans*sulfate (**5**), whereas the corresponding *cis*-compound (**6**) remains in solution; (b) reduction of the isomers to their *leuco* forms (**7** and **8**), with subsequent oxidation, see figure 3. We tried to elucidate the structures of the intermediates **5** - **8**, but could only obtain very limited results.

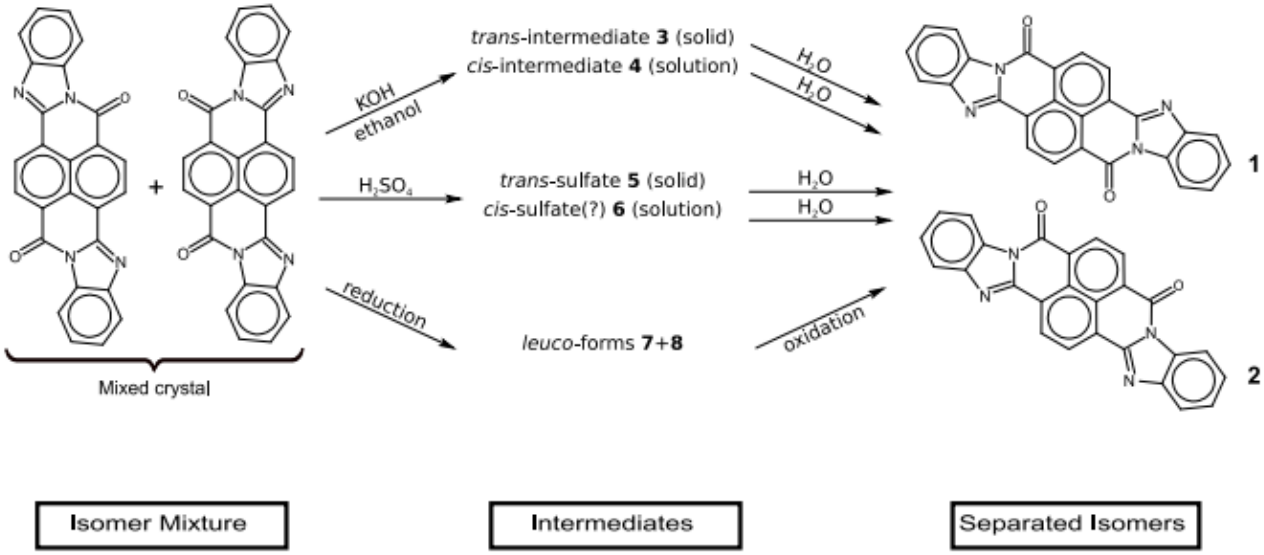

Figure 3: Different approaches for the isomer separation of *trans*- and *cis*-perinone. Hitherto, the molecular structure of all intermediates **3** - **8** were not known. Now, the structures of **3** and **4** were determined.

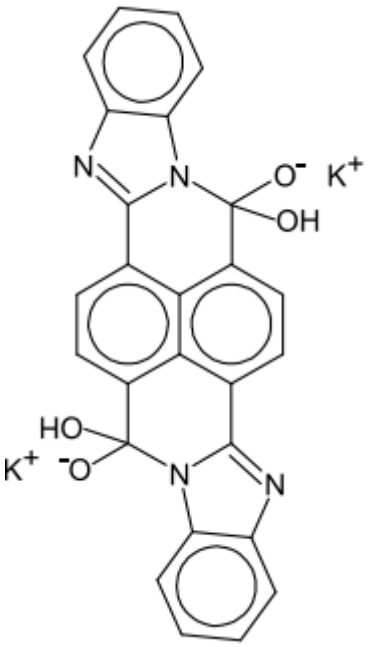

Figure 4: Previously assumed structure of the intermediate **3** as "potassium hydroxide addition product" (**3**).[13]

1.1 Historical

Perinone was first synthesised almost 100 years ago in the laboratories of I.G. Farben (formerly Hoechst AG) in Frankfurt-Höchst, Germany. The corresponding patent was filed in 1924 [3]. The inventors, Wilhelm Eckert and Heinrich Greune noticed, that the reaction of 1,4,5,8-naphthalenedicarboxylic acid with 1,2-diaminobenzene (cf. figure 1) leads to a lucent red powder ("leuchtendrotes Pulver"). The authors were surprised that the product was so deeply coloured, although the starting materials, as well as the imides of 1,4,5,8-naphthalenedicarboxylic acid are colourless. The product could be dissolved in concentrated sulfuric acid, giving a yellow-brown colour. Upon reduction, the product turns green [3].

In the original patent, no statement was made about the constitution of the product. Actually, it was a mixture of *cis*- and *trans*-perinone in a ratio of about 1:1. The industrial production of this mixture started in 1926 [14], i.e. only 2 years after the first patent application. (Apparently, in 1926 the official approval for starting the production of a new chemical compound could be obtained much faster than today). The product was at first sold under the name "Indanthrenscharlach 2G" (Indanthrene Scarlet 2G) [14] and from 1929 as "Indanthrenscharlach GG"[15].(1 The brand name "Indanthrene" was used for many polycyclic pigments, not only for indanthrene derivatives.) It was used as a vat dye for the colouration of cotton and rayon, and for printing on cotton.

In 1926, Eckert and Greune described alternative procedures for the synthesis of the perinone mixture [16,17]. Again, no structural formula was given.

The orange *trans*-isomer was apparently isolated first in 1928. Heinrich Neresheimer from Ludwigshafen and Willy Eichholz from Mannheim described the treatment of the perinone mixture with 320 parts of 60 % H_2SO_4 and 20 parts of chromic acid at 120-125 °C for three hours.[18]

The first method for the separation of the two perinone isomers was invented in 1929 [1]. The approach used a fractional crystallisation from sulfuric acid. The isomer mixture is dissolved in concentrated acid; subsequently, ice is stepwise added, which causes the orange isomer to precipitate as an orange sulfate. The red isomer remains in solution. Alternatively, a hot solution of the isomer mixture in H_2SO_4 can be cooled to room temperature, whereby the orange sulfate precipitates. Hydrolysis in water leads to the final orange product. This patent contains, for the first time, the structural formulae of the two isomers. The molecular formula and the chemical constitution of this "orange sulfate" is not known until today, see Section 3.8.

In 1930, the separation of the isomers by fractionated crystallisation from KOH/ethanol was invented. [1] The isomer mixture is treated with KOH/ethanol (1:7) at 70-80 °C, and subsequently cooled to room temperature. The resulting precipitate (which is the intermediate **3**) is then hydrolyzed to give the orange isomer.

None of these patents state which isomer is the red one, and which is the orange one. This was described by Fierz-David and Rossi in 1938 [14].

The orange *trans*-isomer was sold as Indanthrenbrillantorange GR, whereas the *cis*isomer was described as "bluish-red, quite dull vat dye, which did not gain technical importance" [14].

The perinone isomers were industrially produced at the Hoechst site in Frankfurt am Main. From the spying activities of the US and British secret services in Germany after 1945, it is known that the perinone-isomers were separated using the KOH/ethanol

process: "400 kilograms of potassium hydroxide are dissolved in 2000 kilograms of 90 % alcohol, and then 200 kilograms of Indanthrene Scarlet GG base P [i.e. of the isomer mixture] are added. This is helt for 1 hour at 75 ° and then cooled to 20 °, and the separated potash (The expression "potash" is apparently an error in the FIAT report. The process does not contain potash(K_2CO_3)). addition product is filtered off […]. The nutsch cake is then added into 420 kilograms of 83 % alcohol and 200 kilograms of potassium hydroxide solution are added and again warmed to 75 ° for 1 hour and cooled to 20 °, and again filtered off on the nutsch." The resulting intermediate was subsequently hydrolyzed with water at 60 ° to give the orange *trans*-perinone.[4]

Later, the *cis*-isomer was sold as Indanthrenbordo 2R (1948)[19] and Indanthrenbordo RR (1953)[20].

For many years, both isomers, as well as the mixture, have been used only as vat dyes for cotton. After 1950, the perinones found recognition as pigments. Today, both isomers are produced by Clariant (formerly Hoechst AG) in Frankfurt-Höchst. The *trans*-isomer is sold as Hostaperm Orange GR, and the *cis*-isomer as Novoperm Red TG02.

Despite being such an old product, the synthesis of the perinones is still subject to research. This includes attempts to enhance the yield of the economically interesting *trans*-isomer from 50 % to about 60 %[21] , or to perform the synthesis in a "green", hydrothermal way [22].

The molecular structure and the chemical composition of the intermediate **3**, which precipitates from the KOH/ethanol solution, has never been determined, hitherto. In 1929, the inventors described the intermediate as “KOH compound of the orange isomer”, but the authors explicitly state: “Whether this alkali treatment leads to salt-like compounds, or to addition products, or to molecular compounds, cannot be said”(3 "Ob bei dieser Einwirkung von Alkalien salzartige Verbindungen oder Anlagerungsprodukte oder auch Molekülverbindungen gebildet werden, kann nicht angegeben werden".). This statement remained true for 87 years. The description “KOH addition product” is in use until today. [12] A corresponding molecular formula of a KOH addition product is also used in internal documents of the producer Clariant, see figure 4. [13] However, a search in the archives of Clariant and its predecessor Hoechst AG, did not reveal any analytical investigations supporting this formula. Internally, at Clariant the product is called “Trennsalz” (separation salt), “potassium salt” or “potassium addition product”.

In the following, we show that the intermediate **3** is not the assumed “KOH addition product”, but a salt-like compound of a different molecular formula. A similar structure is also found for the *cis*-intermediate **4**.

1.2 Application

P.O.43 offers a bright orange shade and excellent fastness to heat, light and weathering. *Trans*-perinone thus is a high-price pigment, which is especially used for outdoor applications in plastics, such as tents and awnings. It is also used in paints. [2] P.O.43 is approved in the EU [23] for cosmetic applications except for applications on mucous membranes. It is used as colourant, for example, in soap [24] and nail polish [25]. Its offlabel use in inks for tattoos and permanent makeup is also reported. [26]

P.R.194 and V.R.14 have a duller shade and a good, but not excellent light fastness. Consequently, they are of less commercial interest. They can be used, for example, in paints or as vat dyes.

2. Materials and methods

2.1 Materials

Samples of P.O.43 (**1**), P.R.194 (**2**), V.R.14 (**1+2**) and of the intermediate **3** from the industrial production were provided by Clariant. Solvents and other reactants were obtained from Carl Roth, Fisher Chemical and Sigma-Aldrich and used without further purification.

2.2 Recrystallization and sample preparation of the intermediates 3 and 4

Five different samples of the *trans*-intermediate **3** and two samples of *cis*-intermediate **4** were prepared and investigated. The samples of **3** are denoted as ***A*** to ***E***, the samples of **4** as ***F*** and ***G***.

2.2.1 *trans*-intermediate (3)

Sample ***A*** is the industrial product **3**, obtained from Clariant.

Samples ***B*** to ***E*** were synthesized in-house.

Sample ***B*** was prepared by heating 0.7 g of **1** in a solution of 2 g potassium hydroxide, 5 g ethanol and 0.5 g water. The mixture was stirred at 78 °C for two hours. The resulting yellow precipitate was isolated by filtration and dried in vacuum at room temperature.

Samples ***C***, ***D*** and ***E*** were obtained by recrystallization of ***A*** from a solution containing KOH, water and ethanol in a ratio of 1:2:9 (in the following referred to as "1:2:9-solution"). This solution was used by the German industry before 1945 for the isomer separation of 1 part of perinone.[4]

Sample ***C*** was obtained by recrystallization of 2 g of ***A*** in 5 ml of "1:2:9-solution". The suspension was heated to reflux for three hours, wherein after one and after two hours additional 30 ml of "1:2:9-solution" were added each. This resulted in a yellow solution from which a predominantly fine, pale yellow powder precipitated on cooling. The inhomogeneous crystalline powder was filtered off at room temperature and analyzed by means of powder diffraction. A single-crystal suitable for structure determination could also be picked from the sample.

The filtrate was kept at 4 °C for several months but yielded neither crystals suitable for single-crystal diffraction nor a sufficiently crystalline powder for powder diffraction. Only some thin and very fine deposit on the wall of the vessel could be observed.

Sample ***D*** was prepared for NMR experiments in solution. A deuterated and more dilute analogue of the "1:2:9-solution" was prepared. KOD was synthesized *in situ* by mixing 80 mg potassium dioxide (KO_2) and 0.25 ml deuterium oxide (D_2O) under stirring for ten minutes. Subsequently, 0.75 ml ethanol-d_6 were added. The solution was stored overnight to allow all side-reactions to subside (e.g. formation of deuterium peroxide, which in turn decomposes in alkaline solution to D_2O and oxygen [27]). About 0.5 ml of this solution were used to dissolve a few grains of sample ***A*** and used for solution NMR experiments.

Sample ***E*** was prepared from the already fairly good crystalline sample ***A*** in order to obtain good single-crystals. ***A*** was cured for several hours as suspension in a saturated solution in the "1:2:9-solution" at room temperature, giving single-crystals suitable for Xray analysis.

2.2.2 *cis*-intermediate (4)

Sample ***F*** was prepared by reaction of 1 g of pure **2** with 4 g KOH in 2 g of water and 36 g ethanol under reflux. On cooling to room temperature, a yellow powder precipitated.

Sample ***G*** was prepared by storing a part of sample ***F*** (yellow suspension) in a sealed vessel at 50 °C for 30 hours. The solution turned reddish. Upon cooling to room

temperature, fine needles of **4** precipitated, which were suitable for single-crystal X-ray diffraction.

2.3 Determination of solubility and stability

Solubility experiments were carried out with the sample ***A*** in several solvents at room temperature and under heating to reflux.

2.4 NMR in solution

Perinone is insoluble or almost insoluble in all common solvents, such as $CDCl_3$, benzene or DMSO. The intermediate **3** is either insoluble, or decomposes in solvents. Hence, D_2SO_4 and KOH/ethanol were used to record NMR spectra in solution.
For ^1H and ^{13}C NMR of the intermediate **3** in solution, the sample **A** was dissolved in a solution of deuterated ethanol/KOD as described earlier (Sample ***D***, sect. 2.2).

Measurements were carried out at room temperature on a Bruker AV500 spectrometer operating at 500 MHz for the ^1H nucleus.
Additionally, sample **A** was decomposed with deuterated sulfuric acid and measured directly.
Spectra of solutions of **1** in deuterated sulfuric acid were collected as well. For this measurement, a sample of **1** was synthesized from sample ***A*** by hydrolysis with water, washing and drying.
Measurements in D_2SO_4 were carried out on a Bruker AV500 or on a Bruker DRX600, the latter with a ^1H frequency of 600 MHz.

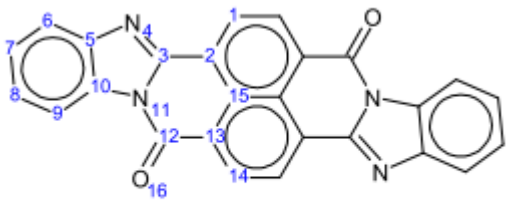

1

Figure 5: Atom numbering for NMR assignment of **1**. Symmetry copies not labelled. For the assignment of the signals, see also [28].

NMR-Signals of **1** in D_2SO_4 (for atom numbering see figure 5):
^1H NMR (D_2SO_4, 500 MHz): 9.85 (d, J = 7.8 Hz, 2H, H1/H14), 9.69 (d, J = 7.8 Hz, 2H, H1/H14), 9.34 (d, J = 8.2 Hz, 2H, H9), 8.60 (d, J = 8.1 Hz, 2H, H6), 8.53 – 8.46 (m, 4H, H7/H8) ppm.
^{13}C NMR (D_2SO_4, 126 MHz): 154.3, 141.1, 131.7, 127.8, 127.6, 127.4, 126.5, 125.3, 122.8, 122.5, 116.8, 113.6, 111.5 ppm.
NMR-data of **3** directly reacted with D_2SO_4 is given in the ESI.
NMR-Signals of **3** in KOD/EtOD (sample ***D***):
^1H NMR (500 MHz, KOD/EtOD): 8,73 (m, 4H, naphthalene), 7.66 (m, 4H, H atoms corresponding to H6/H9), 7.07 (m, 4H, H atoms corresponding to H7/H8) ppm.
^{13}C NMR (126 MHz, KOD/EtOD): 176.64, 163.67, 145.61, 140.07, 135,73, 131.00, 128.47, 126.33, 118.75, 115.78 ppm.

2.5 Infrared spectra

Infrared spectra of **1** and **3** (sample ***A***) were measured to confirm the NMR results. A Shimadzu IRAffinity-1S spectrometer with a Specac diamond ATR-Setup was used. Details and spectra are given in the electronic supporting information (ESI).

2.6 Elemental analysis

Elemental analysis of sample ***A*** gave a composition of
41 % C, 3.7 % H and 6.6 % N.
Calculated for the "KOH addition product" shown in figure 4:
$C_{26}H_{12}N_4O_2 \cdot 4KOH$:
49 % C, 2.5 % H and 8.8 % N.
Calculated for the chemical composition of **α-3** (sample ***E***) as determined by single-crystal X-ray analysis (see 3.5.3):
$K_4[C_{26}H_{12}N_4O_4] \cdot 3C_2H_5OH \cdot 6H_2O$:
45 % C, 5.0 % H and 6.6 % N.
Calculated for the chemical composition of **β-3** (sample ***C***) as determined by single-crystal X-ray analysis (see 3.5.5):
$1.5(K_4[C_{26}H_{12}N_4O_4]) \cdot 5C_2H_5OH \cdot 4\ H_2O$:
49 % C, 4.7 % H and 7.0 % N.
Calculated for **1**:
76 % C, 2.9 % H and 14 % N.
The differences between calculated and experimental values may be caused by the reaction of the hygroscopic intermediate 3 to 1 during the elemental analysis. Additionally, the chemical composition of **3** was assessed gravimetrically: Sample ***A*** was hydrolyzed by water. The resulting orange powder of **1** was filtrated off, washed with water and dried. A weight loss of 52 % could be observed. The expected weight loss on hydrolysis of **α-3** was 51 %. The difference is attributed to impurities in sample ***A*** (K_2CO_3, ethanol) and incomplete recovery of **1** in the filtration step.

2.7 Powder X-ray diffraction

Powder diffraction data were collected on a Stoe Stadi-P diffractometer equipped with a focusing Ge(111) monochromator and a linear position-sensitive detector. Cu-$K_{\alpha 1}$ radiation was employed for all powder measurements. Samples were prepared in glass capillaries with a diameter of 0.7 mm and measured under rotation at room temperature in transmission unless remarked otherwise. The measurement covered a 2θ range from 2 to 80° in steps of 0.2° with 150 seconds per step. Indexing was performed using DICVOL09 as implemented in the program DASH. [29]

2.8 Single-crystal X-ray diffraction

Single crystal X-ray diffraction data of **3** (samples ***C*** and ***E***) were collected on a Stoe IPDS II diffractometer equipped with a Genix microfocus source and mirror optics at 173 K. Mo-$K_{\alpha 1}$-radiation was employed. The data were scaled by the frame-scaling routine in the X-area package[30]. The structure was solved by direct methods using SHELXS and refined by the full-matrix least-squares method using SHELXL.[31] All CH protons of the main molecule were found by difference Fourier synthesis. The hydrogen atoms at the ethanol and water molecules were set to chemical sensible, idealized positions. In **α-3** and **β-3**, all non-H atoms were refined anisotropically. In the case of **4**, data were collected on a Siemens Bruker three circle diffractometer equipped with a Incoatec microfocus source.

Cu-K_α-radiation was employed. The data were scaled by use of SADABS.[32] The structure was solved by direct methods using SHELXS and refined by the full-matrix least-square method using SHELXL.[31] All CH protons of the main molecule were found by difference Fourier synthesis but due to limited data, all H-positions were set to chemical sensible, idealized positions. The crystal quality was quite poor. All non-H atoms were refined isotropically with only one displacement parameter for each ethanol molecule. The atoms linking the main residue with the substituents were constrained to the same displacement as well.

2.9 Solid-state NMR

Preliminary solid-state ^{1}H MAS, ^{13}C and ^{15}N CPMAS NMR spectra of sample ***A*** were recorded on a Bruker (wide-bore) Advance III spectrometer operating at 850, 214 and 86 MHz for the ^{1}H ^{13}C and ^{15}N nuclei, respectively. Samples were packed in 4 mm diameter cylindrical PTFE rotors and spun in a H/C/N-sensitive probe. Different magic angle spinning frequencies were utilized to identify rotational side bands.

Conclusive solid-state NMR spectra of sample ***A*** were acquired on a Jeol ECZR 600 instrument, operating at 600.17 and 150.91 MHz for the ^{1}H and ^{13}C nuclei, respectively. The powder samples were packed in 3.2 mm diameter cylindrical zirconia rotors with a volume of 60 µL and spun at 20 kHz. ^{13}C CPMAS spectra were acquired using a ramp crosspolarization sequence (contact time of 3.5 ms; 90° ^{1}H pulse of 2.1 µs; optimized recycle time of 2.54 s; 4500 scans). ^{13}C MAS (direct excitation magic angle spinning) spectra were acquired with a 90° ^{13}C pulse of 2.15 µs, recycle times of 2 s for 10000 scans. In all spectra, the two pulse phase modulation (TPPM) decoupling scheme with a 119.0 kHz radiofrequency field was used. ^{13}C chemical shifts were referenced to glycine (^{13}C methylene signal at 38.48 ppm) used as external standards.

2.10 Theoretical approaches

Density functional theory has been used with the aim to investigate possible disordered structures and tautomeric states with the program package CASTEP. [33] DFT-D calculations were executed employing the Perdew-Burke-Ernzerhof generalized gradient approximation exchange-correlation density functional and ultra-soft pseudopotentials (cut-off 520 eV; the Brillouin zone is sampled by 1 x 2 x 2 k-points). [34,35] Dispersion correction was done by the Grimme06 model. [36]

The Dreiding force-field [37] was used for model generation for structure determination from powder data and for fast preliminary geometry optimization to locate protons. Infrared spectra were calculated with Gaussian 09 on B3LYP/6-31G* level. [38]

3. Results and discussion

The industrial intermediate **3** has been investigated for its solubility and stability. X-ray powder diffraction revealed the existence of two different crystal phases of **3**, the industrial α-phase (**α-3**) and its pseudopolymorph **β-3**. Single-crystals of both phases could be grown. The crystal structures of both phases were determined by X-ray structure analysis. NMR in solution as well as solid-state NMR provided further information on the intermediate **3**.

The crystal structure of **4** could be elucidated by single-crystal structure analysis as well, resulting in a structure similar to that of **3**.

3.1 Solubility and stability

Samples of **3** and **4** are stable as crystalline powder in dry air. (Dry Argon is even better.)[4] Powder samples of **3** in a closed container in dry air exhibit a reddish orange surface layer after about a

year. Crystals of **3**, stored in a sealed vessel under argon, remain unchanged.)
Suspensions of **3** and **4** in ethanolic KOH are stable as well. (The suspensions remained unchanged over several weeks.) In contact with moisture or
CO_2, the pale yellow intermediate **3** is converted to the orange *trans*-perinone **1**.
Analogously, the nearly colourless powder of **4** is converted to the red *cis*-perinone **2** in contact with water.
Keeping a suspension of the *trans*-perinone **1** in KOH/ethanol at room temperature leads to slow conversion of **1** to **3** within several days.
Samples of **3** tend to be inhomogeneously coloured with shades from pale yellow to almost colourless. The yellow colour presumably arises from minute contamination, e.g., with traces of **1**.
According to literature, the intermediate **3** should have a modest solubility in ethanol. [12] Apparently, this is only valid if the solution contains a significant amount of KOH.
In most solvents, **3** easily reacts to **1** in the absence of potassium hydroxide. Even pure ethanol(6 "Ethanol, absolute" by Fisher Chemical (99.8+ %) and "Rotipuran® Ethanol, absolute" by Carl Roth (≥ 99.8 %), both with comparable results.
) or methanol seems sufficient as reaction partner, as a bright orange to red color develops in mixtures of these alcohols with **3**. The observed reaction in "pure" alcohols could also be attributed to traces of water in the solvent or admission of moisture from air.
In a mixture of ethanol and KOH (5:1 by weight), **3** has a solubility of 6 to 10 g/l at room temperature.
The measured solubility of **3** in KOH/ethanol is adulterated by impurities from the crystallization process (e.g. excess potassium hydroxide or solvent). Adsorbed ethanol on the crystals increases the apparent solubility. The solubility is reduced by the presence of CO_2 which reacts with KOH and results in K_2CO_3. The potassium carbonate sometimes even form fairly large crystals, especially in aged samples or samples that were not handled with all of the appropriate care. Also the first single-crystal, which we found in a sample of **3** and analysed by X-ray structure analysis,
turned out to be K_2CO_3 instead of **3**.
At higher temperatures, the solubility in KOH/ethanol increases slightly. No attempt was made to quantify this temperature dependency.
Both isomers of perinone (**1** and **2**) can be dissolved in concentrated sulfuric acid under protonation. Both isomers give reddish brown solutions [7]. The structures of the protonated species are not known (See sect. 3.8).

3.2 NMR in solution

The ^{13}C NMR spectrum of **1** in D_2SO_4 shows 13 peaks. This is in agreement with the centrosymmetry of the molecule containing 26 carbon atoms. The ^{1}H NMR spectrum agrees with the centrosymmetry, too. The NMR spectra of *cis*-perinone in D_2SO_4 confirm the mirror symmetry (C_{2v}) of the *cis*-isomer.
The NMR spectra were also used to confirm the isomer purity of **1**. Signals of the *cis*isomer were not present, confirming that our sample of **1** contained the *trans*-isomer only.
The intermediate **3** (sample ***A***) was reacted with D_2SO_4. The resulting solution had the same reddish-brown colour as a solution of **1** in D_2SO_4. Both solutions contained similar peaks in the ^{1}H NMR spectrum, but the peaks were shifted. In the D_2SO_4 solution of **3**, additional signals were observed, which were attributed to ethanol molecules and traces of diethyl ether (which results from the reaction of ethanol with D_2SO_4). Other impurities

in the sample were not investigated in further detail. The overall shift of the peaks results from dilution of the D_2SO_4 by water. [39] These observations indicated that the intermediate **3** contains ethanol and water molecules in the crystal lattice.
^1H ,^{13}C (^1H gated decoupling) as well as $^1H/^{13}C$-NMR spectra of **3** were recorded in KOD/ethanol-d_6 (sample ***D***). The unusual solvent rendered comparisons with literature data difficult. The ^{13}Cspectra in KOD/ethanol contained only 10 signals (in contrast to 13 signals in D_2SO_4), which is in clear disagreement with the assumed formula of **3** depicted in figure 4. These findings are interpreted in sections 3.5.1 and 3.5.2.

3.3 Crystal phases

3.3.1 Crystal phases of the *trans*-intermediate (3)

The X-ray powder patterns of different samples of the intermediate **3** show, that there are actually two different phases, which we call α and β. The α phase is obtained in the industrial production (sample ***A***).
Sample ***B***, which was obtained by heating P.O.43 in suspension in KOH/ethanol at 78 °C (see sect. 2.2), consisted of poorly crystalline **α-3** and some impurities.
β-3 is formed by recrystallization of sample ***A*** in a boiling mixture of KOH, water and ethanol (1:2:9) (sample ***C***).
In contrast to the described phase transition on recrystallization from "1:2:9-solution", keeping powder samples of **α-3** or crystals of **α-3** suspended in the "1:2:9-solution" at room temperature retains the α-phase (sample ***E***).

3.3.2 Crystal phases of the *cis*-intermediate (4)

Sample ***F***, which was obtained by dissolving P.R.194 in KOH/ethanol at reflux, followed by cooling to room temperature (see sect. 2.2), consisted of **4** and some impurities, as shown by PXRD. Most probably, there are more phases of **4**. The powder pattern of sample ***F*** shows peaks not attributable to the single-crystal structure of **4** (which was determined from crystal needles from sample ***G***). Furthermore, amorphization of the sample ***F*** could be observed in dry air. This holds true for crystals from sample ***G*** as well[8], indicating a desolvation, and the existence of an ansolvate or an solvate with lower solvent content.

3.4 Attempted structure determination of 3 from powder data

The industrial sample **A** of the *trans*-intermediate **3** is a well-crystalline powder, but did not contain single-crystals suitable for X-ray structure analysis. Therefore, attempts were made to determine the crystal structure from powder data.
The X-ray powder diffractogram of sample ***A*** (α-**3**) was of good quality. The diffractogram was successfully indexed with a monoclinic unit cell with cell parameters of a = 27.7 Å, b = 12.3 Å, c = 12.1 Å and a monoclinic angle of β = 107°. The systematic extinctions pointed to $C2/c$ as most likely [40] space group. A successful Pawley refinement confirmed the cell parameters and the space group. [40,41]
Structure determination was tried by the real-space method with simulated annealing.[29] Since the exact molecular structure of **3** was not known at that time, different molecular models were tested. All of them contained the molecule as “potassium hydroxide addition product”, as depicted in figure 4, in the di-anionic or tetra-anionic state. All molecular models were optimized with the DREIDING force field [37], in order to assure a sensible molecular geometry. The structure solution trials were run with different molecular models and varying numbers of ethanol and water molecules. All

attempts invariably failed. No crystal structure was found which matched the experimental powder pattern.
After the structure had been solved by single-crystal X-ray diffraction it became obvious, that the structure solution from powder data failed, because the assumed molecular model was wrong. The actual molecular geometry, described in 3.5.1, dissented too much from the model which was used in the simulated annealing.

3.5 Crystal structures of the *trans*-intermediate (3)

The crystallization experiments, described in section 2.2, yielded two different singlecrystals, suitable for structure determination by single-crystal X-ray diffraction. Both crystallizations started from the industrial sample ***A*** (see figure 6 left). Single crystals of the α-phase of **3** could be obtained by curing the sample ***A*** in a mixture of KOH, water and ethanol (1:2:9) for several hours at room temperature (Sample ***E***). Recrystallization of sample ***A*** from the same solvent mixture at reflux led to the formation of single crystals of the β-phase (Sample ***C***, figure 6, right).
The α-phase (sample ***E***) corresponds to the industrial phase.
The crystal structures of both phases were determined by single-crystal X-ray diffraction (for details see ESI).

[8] The amorphization of ***G*** could be observed several times on the diffractometer, because dry nitrogen is used to cool the single crystals during the X-ray. The crystals decompose, but no red colour is observable. This indicates a desolvatation, but no reaction of **4** to **2**.

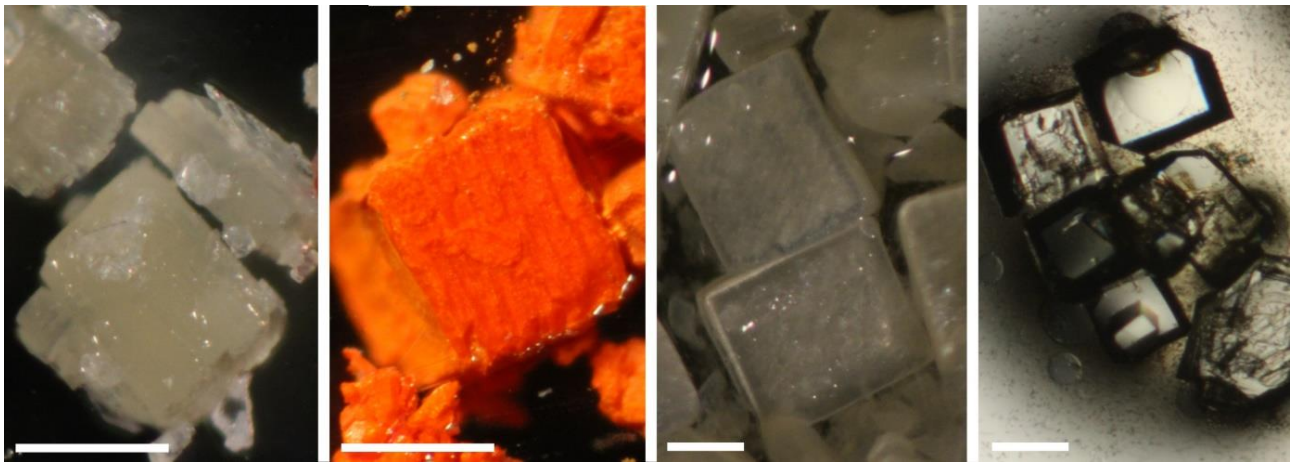

Figure 6: Sample ***A*** from industrial production (α-**3**, left), (slowly) hydrolyzed sample ***A*** (second left), Sample ***E*** (α-**3**, third left) and crystals from sample ***C*** (β-**3**, right). Upon hydrolysis, the grain shape is mostly retained (middle). The white bars in the images have a length of about 100 µm.

Both crystal structures contain in their lattices the organic anion ("perinone anion"), potassium cations, ethanol and water molecules. The structures of the two phases (α-**3** and β-**3**) differ in their water and ethanol contents. The main common feature is the chemical structure of the "perinone anion".

3.5.1 Chemical structure of the *trans*-intermediate (3)

The single crystal X-ray analysis of the α- and β-phases of the *trans*-intermediate **3** revealed, that **3** is not the "potassium hydroxide addition product" depicted in figure 4. In contrast, the crystal structures show that, surprisingly, the conversion of **1** to **3** is accompanied by unexpected ring openings (figure 7). The two lactam groups (N–CO) disconnect by cleavage of the bond between C12 and N11, and carboxylate groups are formed, see figure 7.
Upon hydrolysis of **3** with water or dilute acid, the lactam bond is reconnected and the perinone is restored.

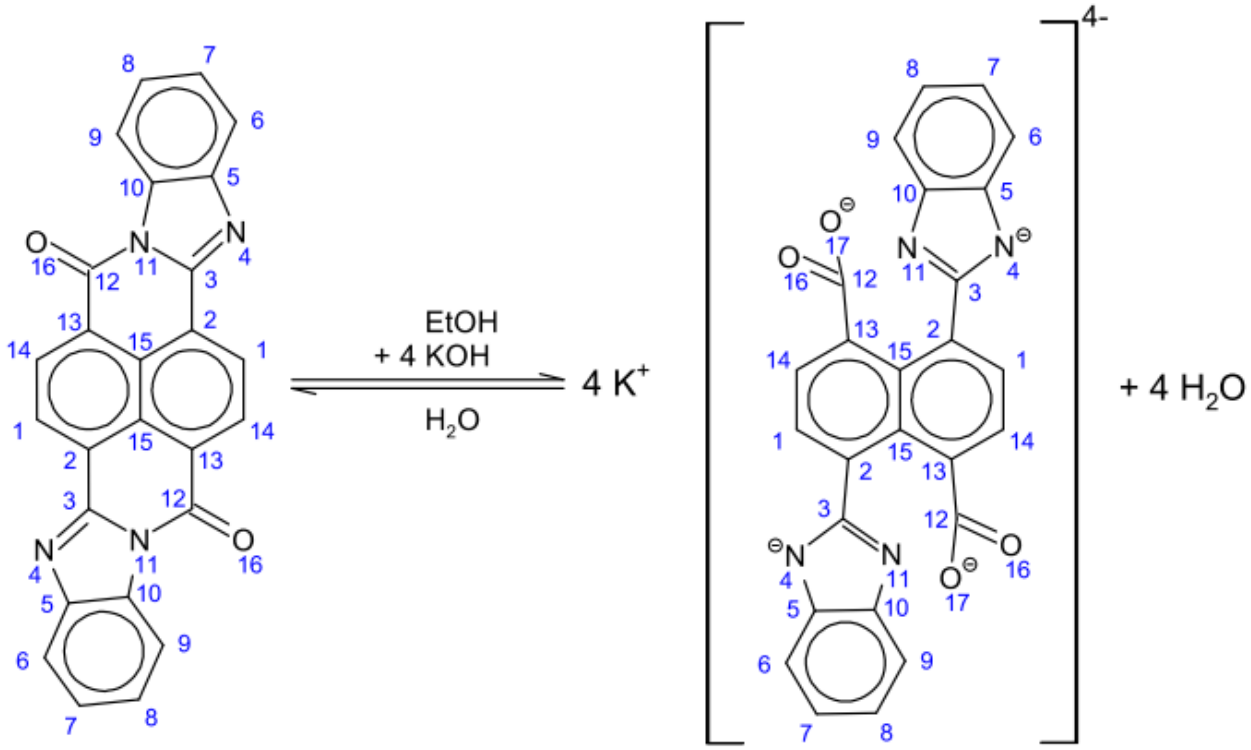

Figure 7: Molecular structure of the intermediate **3** (right), and reaction from **1** to **3**, with atomic numbering.

3.5.2 On the protonation state of 3

From the single-crystal X-ray data of **α-3** and **β-3**, no distinctive conclusion on the protonation state of the organic anion (specifically of N4 or N11) could be drawn. The crystal structures of the α- and the β-phases of **3** contain four potassium cations per perinone anion. Correspondingly, there must be four negative counter-charges. There are two possible cases:
Case I: The two carboxylate groups and the two benzimidazole groups are deprotonated, leading to the tetra-anion shown in figure 7 and in figure 8, case I.
Case II: The benzimidazole groups are not deprotonated, but contain a N-H group each, leading to a di-anion. To compensate for the charge of the potassium cations, two ethanol molecules per organic anion must be deprotonated (see figure 8, case II).
From the viewpoint of an organic chemist, both cases look chemically reasonable. In such cases, a consideration of the pK_a values should be helpful. However, the pK_a values of the perinone di-anion are unknown. The experimental determination of the pK_a values of **3** in

solution is hampered by the instability and limited solubility of **3**. Theoretically, the pK_a values could be calculated; but pK_a values, calculated in the gas phase or in solution, do not necessarily reflect the situation in the solid-state environment. The same holds for experimental pK_a values.
In the crystal structures, there is a short contact between the atom N4 of the benzimidazole and the oxygen atom of an ethanol molecule (compare figure 9 on page 23 and figure 17 on page 32). Obviously there is a hydrogen bond. This could either be a N⊖···H-O bond (case I) or a N-H···⊖O bond (case II), see figure 8.

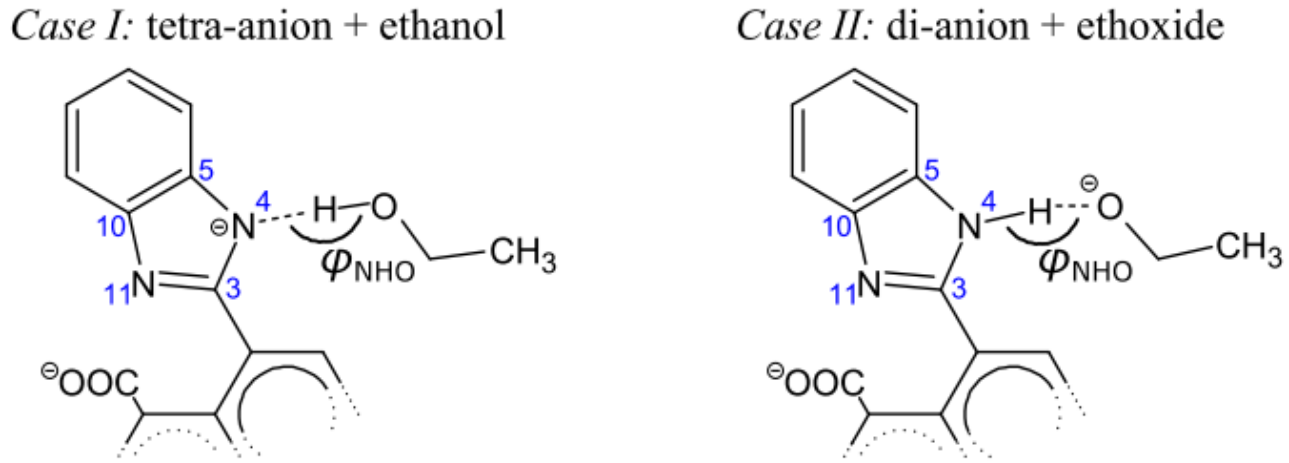

Figure 8: Possible protonation-states of **3**.

From the X-ray data of α-**3** and β-**3**, the position of the hydrogen atom in question could not be localized in the difference fourier maps because of limited crystal quality.
In case II, the bond lengths C3-N4 and C3-N11 should differ by about 0.05 Å (CSD-Search with Mogul [42]), whereas they should be about equal in length in case I. Experimentally, their two bond lengths are equal within the precision of the measurements. This holds true for **α-3** as well as for all corresponding bond lengths of the three symmetrically independent fragments in **β-3** (see table 1). This points to case I. Similarly, the bond lengths C5-N4 and C10-N11 should differ by about 0.02 Å for case II, whereas they should be roughly equal in case I. Also here, all experimental values point to case I.

Table 1: Bond lengths (in Å) between nitrogen and carbon in the benzimidazole system, expected for case I and case II (CSD data), in comparison to the experimental values.

	CSD mean values		experimental			
bond	case I[1]	case II[2]	**α-3**	**β-3** frag. 1	**β-3** frag. 2	**β-3** frag. 3
C3-N4	1.35(4)	1.36(3)	1.354(3)	1.349(8)	1.339(7)	1.347(8)
C3-N11	1.34(4)	1.31(4)	1.341(3)	1.347(8)	1.357(7)	1.347(7)
Δ	0.01	0.05	0.013	0.002	-0.018	0.000
C5-N4	1.36(4)	1.43(5)	1.381(3)	1.389(8)	1.374(7)	1.390(8)
C10-N11	1.37(4)	1.45(5)	1.393(3)	1.391(8)	1.393(7)	1.391(8)
Δ	-0.01	-0.02	-0.008	-0.002	-0.019	-0.001

[1] CSD-search fragment: C_{cycl}-$N^{\ominus}$-C-N(H_0)-C_{cycl} (223 hits).

[2] CSD-search fragment: substituted imidazole (139 hits).

The geometry of the hydrogen bond was investigated as well. The H atom in question was placed in a calculated position either at the O atom (case I) or at the N atom (case II). For case I, the N⊖···H-O angle is roughly 180°, which is a typical value for hydrogen bonds. For case II, the N-H···⊖O angle is between 120 and 155°, which is quite uncommon for a reliable hydrogen bond (see table 2). Hence, these angles are a clear argument for case I. The angle N···O–C, incorporating the CH_2 group of the ethanol molecule, should be about 111 ± 14° for case I [9], and 119 ± 14° for case II [10], which is not a significant difference. The experimental values (table 2) are closer to 111°, which is a weak favour for case I.

Table 2: Angles in the hydrogen bond between an N atom of the benzimidazole group and an ethanol molecule case I and case II in **α-3** and **β-3**. Hydrogen atoms on calculated positions.

phase	angle	case I φ(N···H–O) / °	case II φ(N–H···O) / °	both cases φ(N···O–C) / °
α-3	N4-H-O1E	128.8	179.4	113.7(6)
β-3[1]	N4A-H-O41E	155.4	173.6	104.7(6)
	N4-H-O21E	152.0	179.9	105.6(7)
	N4B-H-O51E	97.2[2,3]	179.5	109.1(8)
	N11B-H-O31E	120.3[2]	179.7	104.6(6)

[1] Three symmetrically independent fragments. In the third fragment both atoms N4 and N11 have a close contact to an ethanol molecule.

[2] H atom either at N4B or N11B.

[3] No H bond.

Another minute, yet productive argument in favour of case I is, that all hydrogen atoms of the C-H groups of the perinone anion could be located by difference fourier synthesis, but no H atom was found at the N atoms. The hydrogen atoms of ethanol and water molecules could not be located reliably from the X-ray data, because the ethanol and water molecules are disordered, as visible from the larger thermal parameters, from the reduced occupancies of several atoms, and from the solid-state NMR experiments (see Sect. 3.5.3.). Hence, the proton of the OH group of the ethanol molecule cannot be expected to be found in any case. Therefore, the inability to locate the proton of the N-H-O hydrogen bond is an argument for case I.

In the solid-state infrared spectra, no N-H-bands could be observed. In addition, no ethoxide could be detected. *Ab initio* calculations were employed to generate reference IR

spectra, but the resulting gas-phase spectra were not comparable to the measured solidstate spectra. Hence, the IR spectra gave a fade hint in favour of case I.

[9] CSD search fragment: N···H–O–CH_x with: N having aromatic bonds to two C atoms), x = 2,3 and d(N...O) ≤ 3.27 Å. 2075 hits, CSD mean value 110.6° ± 13.8°
[10] CSD search fragment: N–H···O–CH_x with: N having single bonds to two C atoms), x = 2,3 and d(N...O) ≤ 3.27 Å. 6230 hits, CSD mean value 119.4° ± 13.5°

The ^{1}H NMR spectra of **3** in ethanol-d_6/KOD did not contain signals of N-H, but also in case II these signals would not be visible due to a rapid exchange of the H atom with the deuterated solvent.
The ^{13}C NMR spectra of **3** in ethanol-d_6/KOD solution showed only ten signals. This finding proves the magnetic equality of the atom pairs C5/C10, C6/C9 and C7/C8 of the benzimidazole group. Thus, either both nitrogen atoms (N4 and N11) are not protonated or a fast exchange takes place since the attached carbons act magnetically equivalent. Hence, the ^{13}C NMR spectra show that the intermediate **3** has a ring-opened structure not only in the solid, but also in KOH/ethanol solution. The protonation state in solution remains obscure.
Solid-state NMR (^{1}H, ^{13}C and ^{15}N) provided no clear answer on the protonation state.[11]
DFT-D calculations were set up to determine the protonation state of **α-3**. Several attempts were made: (1) optimization of the whole unit cell; (2) optimization of only the ethanol molecules; (3) optimization of only the proton position of the N···H···O hydrogen bond in the otherwise fixed structure. (4) Several approaches with different numbers of ethanol and water and (5) approaches with super cells and different numbers of ethanol and water. All approaches gave no decisive results or were far too expensive in terms of computing time. The optimizations of the whole unit cell did not converge, probably due to disorder or dynamics. Super cell calculations, set up to account for partly occupied solvent positions proved not feasible. Calculations with a moveable proton between O1E1 and N4 in an otherwise fixed structure favoured a N···H–O bridge rather than a N–H···O bridge, but the energy difference was rather small.

3.5.3 Crystal structure of the industrial α-phase of 3 (α-3)

Single-crystals of the industrial phase **α-3** have been obtained by curing sample ***A*** in 1:2:9-solution (sample ***E***, Sect. 2.2). The crystal structure has successfully been determined at 173 K (figure 9). This crystal structure corresponds to the industrial product. This was confirmed by comparison of a simulated powder pattern of **α-3** with an experimental powder diagram of the industrial sample (sample ***A***), both measured at 173 K (see figure 10).

[11] Solid-state ^{15}N spectra were recorded overnight. The samples turned orange, visually indicating a reaction of **3** to **1** during the measurement. Three weak peaks were observable. They might be interpreted as two signals from **1** and one signal from **3**, which is an indication for the magnetic equivalence of the two N atoms of the benzimidazole group, which could, however, also be caused by dynamical effects in case I or case II.

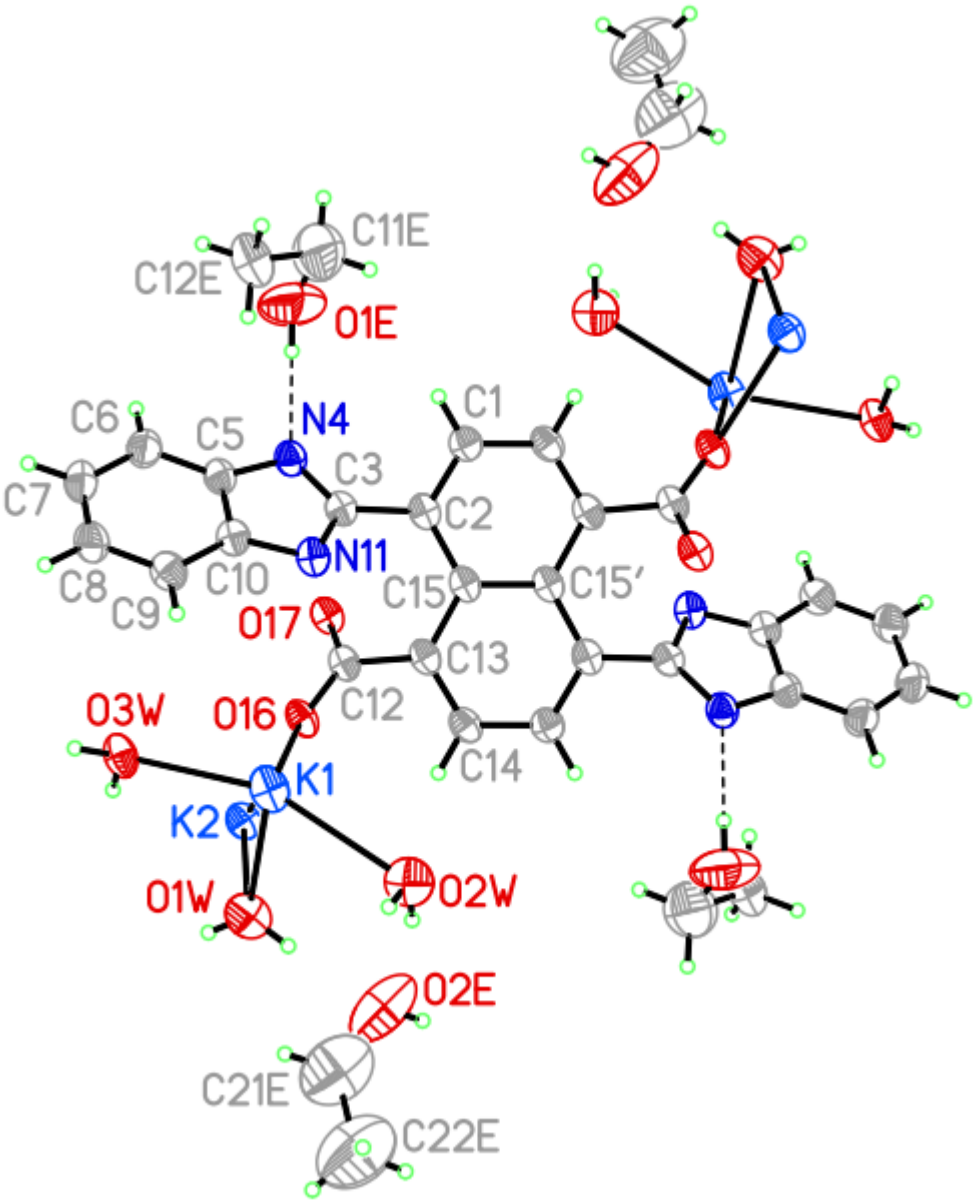

Figure 9: Ellipsoid plot (50 % probability) of **α-3**. Symmetry copies generated by the crystallographic inversion centre at the centre of the molecule are not labelled. For C11E and C12E only the major occupied positions are shown. The O–H···N bonds are shown as dotted lines.

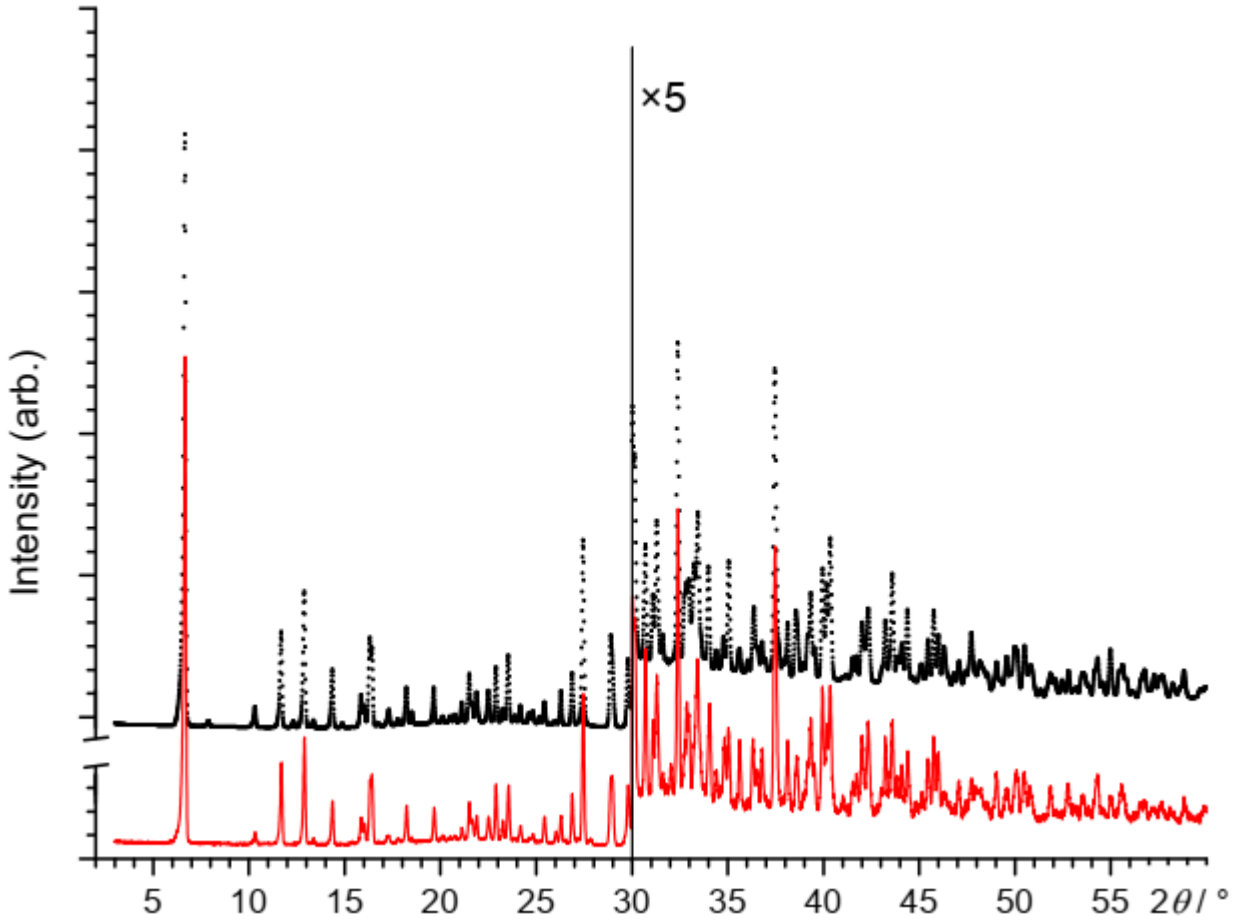

Figure 10: Experimental powder pattern of sample ***A*** (untreated industrial sample; black) and simulated powder pattern of **α-3** (red). Both measurements, powder and single crystal, were performed at 173 K.

Compound **α-3** crystallizes in the monoclinic system. A unit cell with the dimensions a = 27.6799(16) Å, b = 12.3372(5) Å, c = 12.0253(7) Å and β = 106.951(4)° (at 173 K) has been found, which corresponds to the values obtained by X-ray powder diffraction. The unit cell volume is 3928.1(4) Å^3 at 173 K. The space group was determined as $C2/c$, as already found by X-ray powder diffraction. Further crystallographic details are given in in table 3.

Table 3: Crystal structural data of the intermediates α-**3**, β-**3**, and **4**.

Compound	**α-3** *(trans, industrial phase)*	**β-3** *(trans)*	**4** *(cis)*
Chemical composition	$K_4[C_{26}H_{12}N_4O_4]$ · $3C_2H_5OH$ ·$6H_2O$	$1.5(K_4[C_{26}H_{12}N_4O_4])$· $5C_2H_5OH$·$4H_2O$	$K_4[C_{26}H_{12}N_4O_4]$ ·$3C_2H_5OH$·$3H_2O$
Formula	$C_{32}H_{42}K_4N_4O_{13}$	$C_{32.67}$ $H_{37.33}$ K_4 N_4 O_{10}	$C_{32}H_{36}K_4N_4O_{10}$
M_r	847.09	802.40	793.05
Crystal system	monoclinic	triclinic	monoclinic
Space group	*C* 2/*c*	*P*-1	14 (*P* 2_1/n)
Z, *Z'*	4,0.5	3,1.5	4, 1
T / K	173	173	293(2)
a / Å	27.6799(16)	9.7342(9)	6.586(2)
b / Å	12.3372(5)	16.3726(15)	34.99(2)
c / Å	12.0253(7)	19.1558(17)	16.636(19)
	90	68.834(7)	90
β / °	106.951(4)	84.851(7)	102.11(6)
	90	77.963(7)	90
V / Å3	3928.1(4)	2784.0(5)	3748(5)
ρ_{calc} (Mg · m^{-3})	1.432	1.436	1.405
Crystal habit	block	block	thin flat needles
Crystal colour	light brown	light brown	colourless
Crystal size / mm	0.28 × 0.28 × 0.25	0.26 × 0.26 × 0.23	1 × 0.1 × 0.05
Radiation	MoKα	MoKα	CuKα
λ /Å	0.71073	0.71073	1.54178
Θ range / °	2.379 – 26.901	2.058 – 25.566	2.526 - 33.289
№ of meas. refl.	18813	25658	9272
R_{int}	0.0313	0.0611	0.2212
$R[F^2>2\sigma(F^2)]$	0.0536	0.0946	0.0986
$wR(F^2)$	0.1509	0.2725	0.2589
S	1.050	1.065	1.049
№ of reflections	4224	10220	1361
№ of parameters	294	685	204
№ of restraints	84	134	16
$\Delta\rho_{max}$	0.770	1.063	0.626
$\Delta\rho_{min}$	-0.532	-0.773	-0.746

The unit cell contains four perinone-anions, which are situated on crystallographic inversion centres. The asymmetric unit is composed of half a perinone tetra-anion, two potassium cations, one and a half molecules of ethanol and three water molecules. Hence the chemical composition of the industrial intermediate is: $K_4[C_{26}H_{12}N_4O_4]$ ·$3C_2H_5OH$·$6H_2O$.

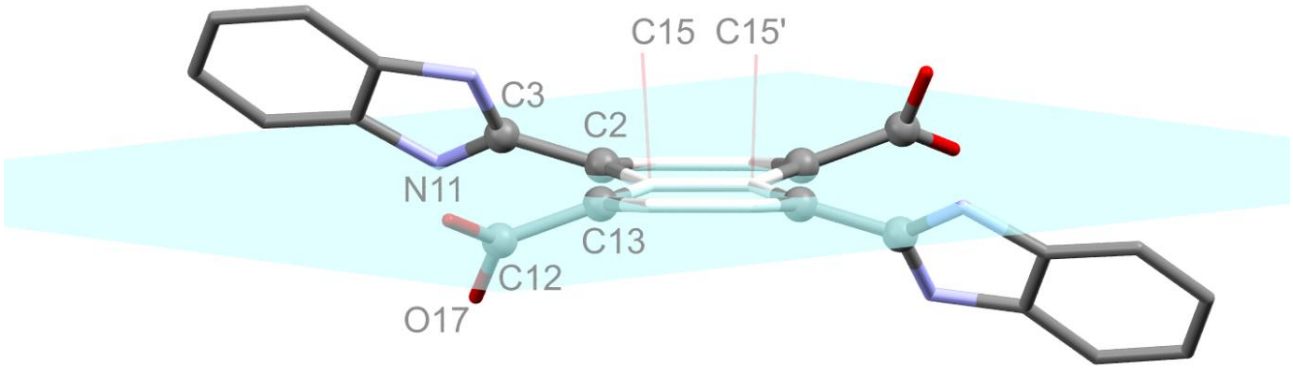

Figure 11: Organic anion in **α-3**. Mean plane (light blue) of the six central naphthalene carbon atoms depicted in white. The naphthalene system and its substituents are nonplanar. which is well visible from the carbon atoms depicted as grey balls.

The organic tetra-anion is composed of a central naphthalene system, which is tetra substituted in 1,4,5,8-position by two benzimidazolate and two carboxylate substituents. There is a strong intramolecular repulsion between the neighbouring substituents, caused by steric requirements and by the Coulomb repulsion between the negatively charged carboxylate and benzimidazolate groups. This leads to a distortion of the molecule in two ways: (1) a rotation of the four substituents against the naphthalene plane, (2) an out-of-plane bending of the substituents causing a deformation even on the naphthalene system itself.
Ad (1): The carboxylate group is rotated against the naphthalene plane by 34.7(3)° as manifested by the torsion angle φ(O17–C12–C13–C15). The neighbouring benzimidazole is rotated in the same direction by 39.2(3)° (φ(N11–C3–C2–C15)), see figure 11.
Ad (2): The naphthalene system deviates by 0.035 Å RMS from its mean plane. The carbon atoms C13 and C2 are by 0.12 Å below and above the mean plane. The carbon atom of the carboxylate moiety (C12) is 0.63 Å below this plane and the bonding carbon atom of the benzimidazolate (C3) is 0.55 Å above (see figure 11). The corresponding torsion angles are φ_1(C12-C13-C15-C15') = 157.2(2)° for the carboxylate group, and φ_2(C3-C2-C15-C15') = 160.7(2)° for the benzimidazolate group (figure 12). A CSD search for 1,4,5,8-tetrasubstituted naphthalene compounds was performed. In case of aliphatic substituents, the naphthalene system is almost planar ($\varphi_1 = \varphi_2 = 180°$). For aromatic substituted naphthalenes, torsion angles between 155° and 167° are frequent (see figure 12). Hence, the perinones geometry is no outlier.

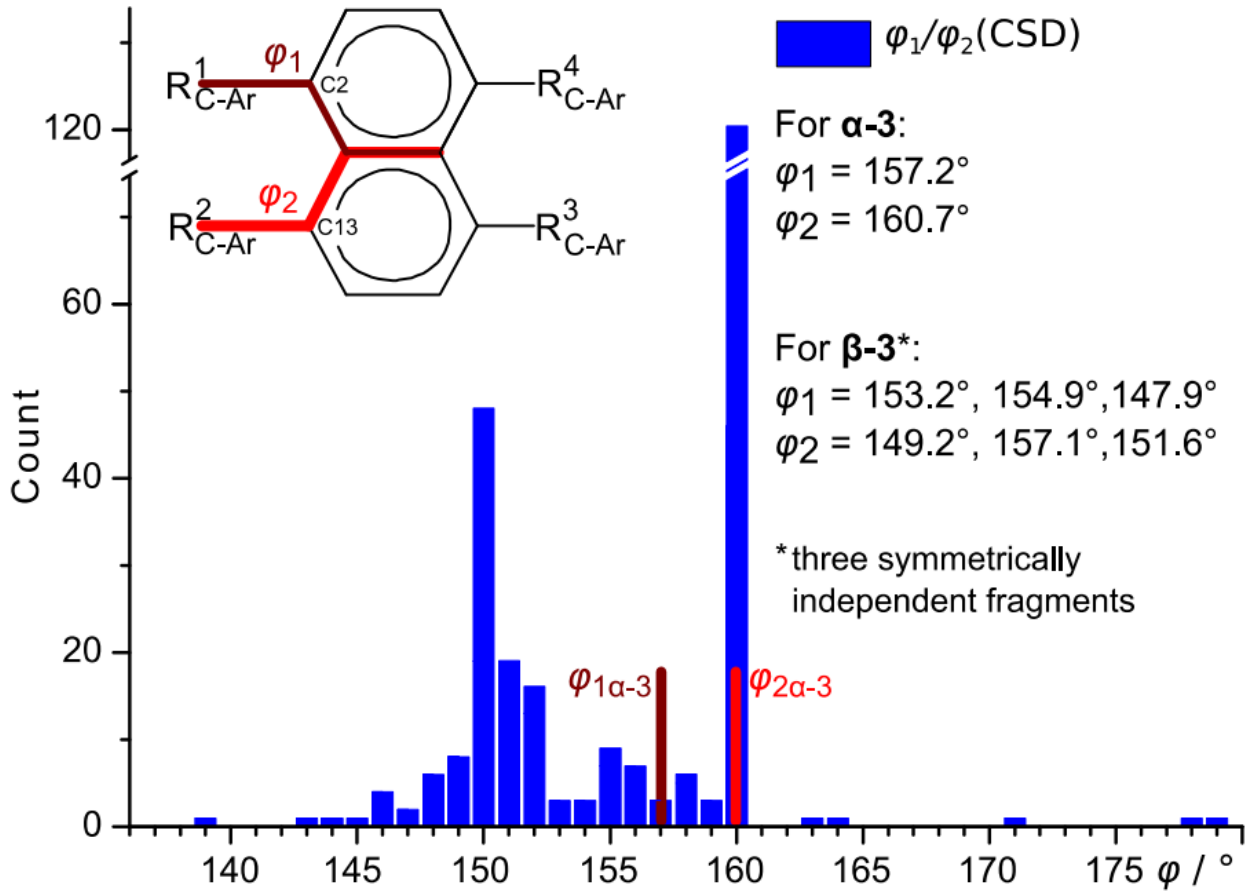

Figure 12: Distribution of torsion angles of 1,4,5,8-tetrasubstituted molecules in the CSD. The inset shows the CSD query motif. The CSD search was restricted to only aromatic substituents R_1-R_4. In the experimental structures of α-3 and β-3, R_1 and R_4 are the COO- groups and R_2 and R_3 the benzimidazolate groups.

The benzimidazolate mean plane forms a dihedral angle of 44.5° with the naphthalene mean plane. Similarly, the carboxylate plane forms a dihedral angle of 46.2° with the naphthalene's mean plane (figure 14).
Those rotations are caused by steric requirements and by the Coulomb repulsion between the negatively charged benzimidazolate and carboxylate groups.
Because of the nonplanarity, the electronic conjugation between the π-systems of the naphthalene group and the π-systems of the carboxylate and the benzimidazolate groups is strongly hampered. The interrupted conjugation explains the colour differences between the bright orange perinone **1** and the almost colourless intermediate **3**.
Also the π-stacking of neighbouring molecules, which generally contributes significantly to the colour of organic pigments, is hindered by the strong out-of-plane bending of the benzimidazolate fragments. Actually, the distance between neighbouring naphthalene centres is more than 8 Å.

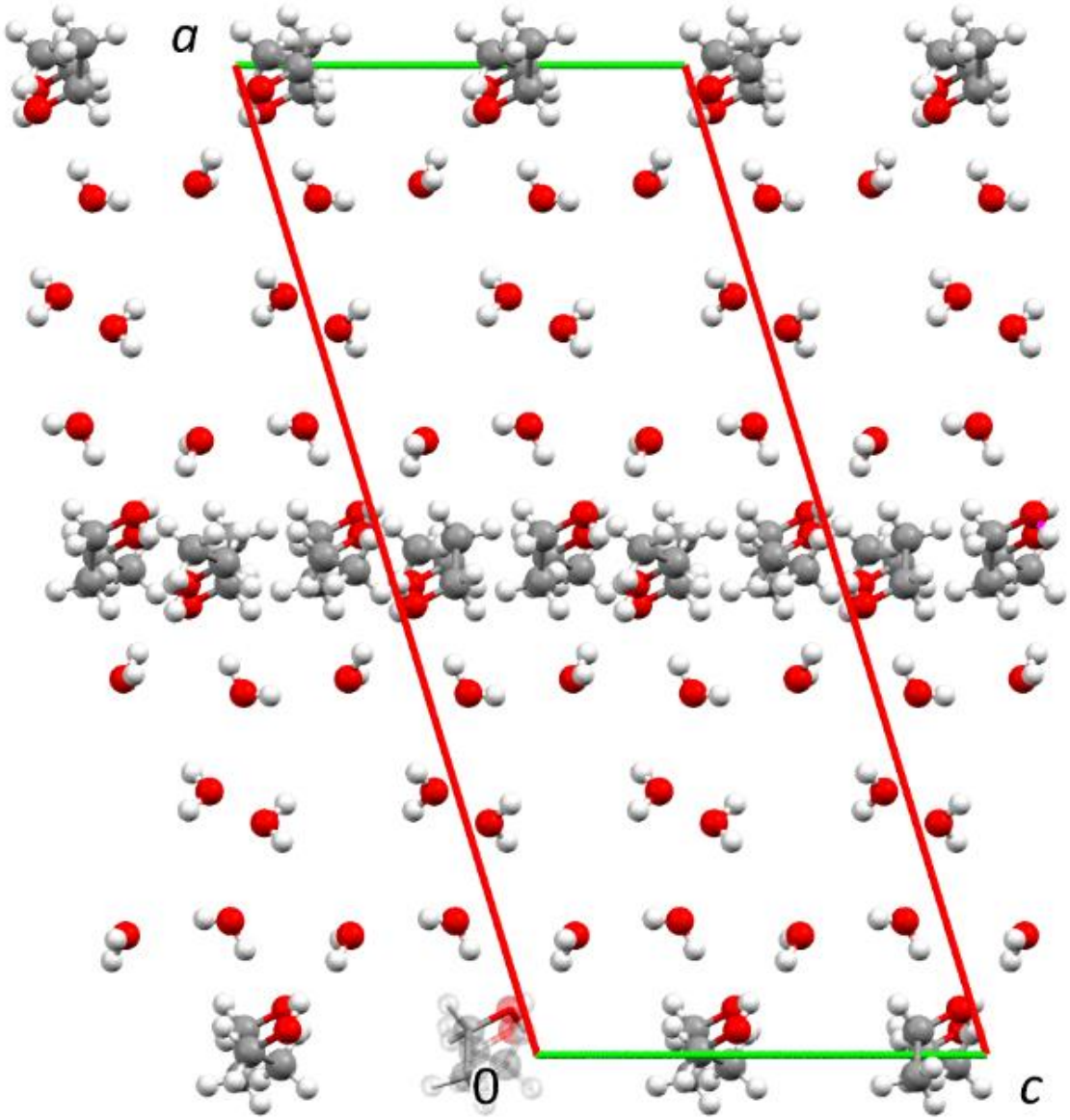
a
0
c

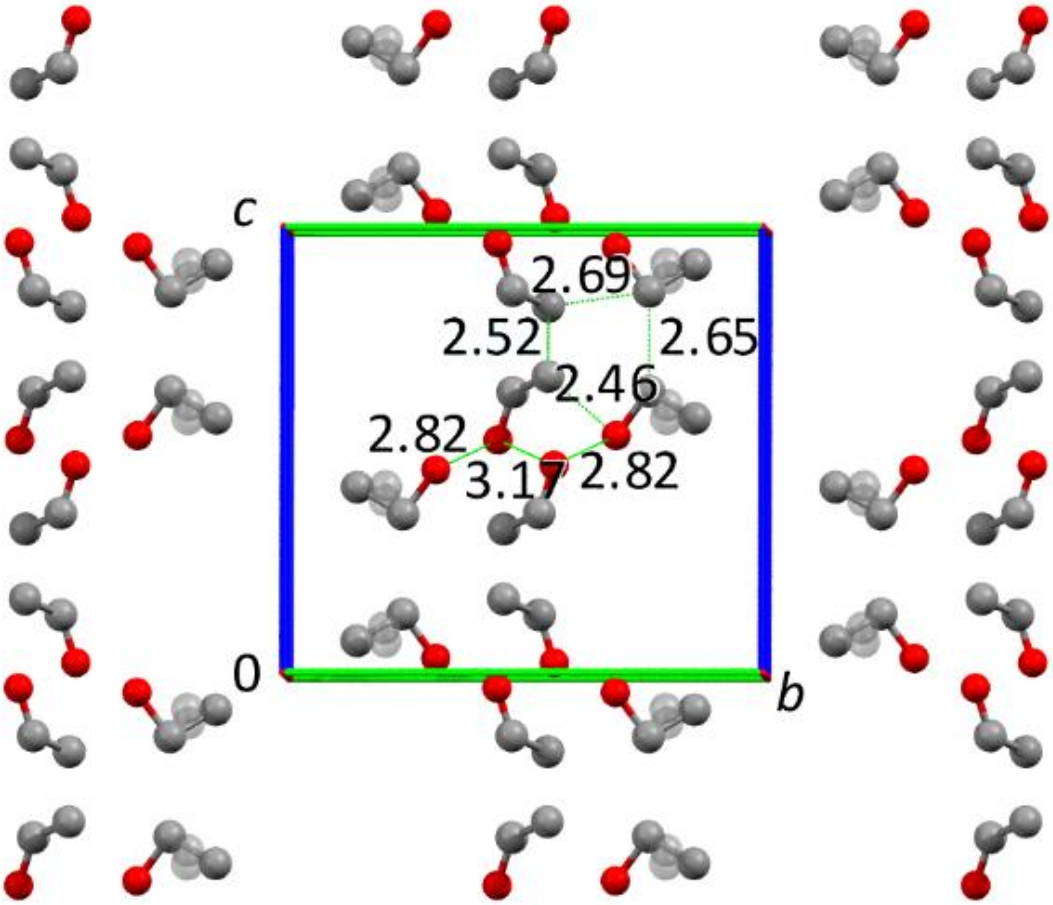

Figure 13: Arrangement of ethanol and water molecules in **α-3**. (top) View along the *b*-axis. Only major occupied positions of disordered positions are shown. (bottom) Arrangement of the
ethanol molecules in the ethanol layer. View along the *a*-axis. The numbers show the short intermolecular distances between C and O atoms of the ethanol molecules. O···O distances of 2.8-3.1 Å are typical for hydrogen bonds, but O···C and C···C distances of 2.5-2.7 Å are only possible between average positions in highly dynamic or disordered systems. The minor occupied atomic positions are drawn more transparent.

The structure contains two symmetrically independent potassium cations, both on a general position. The first potassium ion (K1) is six-fold coordinated by the carboxylate groups (η_1) of two anions, by three water molecules and by the π-system of the naphthalene system of one anion (figure 14). The second cation (K2) is six-fold coordinated as well. It coordinates two-fold to the carboxylate (η_2) and the benzimidazoles π-system of one anion, to the carboxylate group (η_1) of another anion, and

to two water molecules (figure 14). Astonishingly, the potassium cations do not coordinate to the negatively charged N atoms of the benzimidazolate fragments.
All water molecules in the structure are coordinated to potassium anions. The water molecules are arranged in channels parallel to the *c*-axis around the K_+ ions, see figure 14. The most prominent hydrogen bond pattern in the structure is a second level $C_{44}(22)$ chain, linking the carboxylate moiety of one organic anion to the benzimidazole nitrogen (N4) of another via a water molecule.[43,44]
Both ethanol molecules are disordered. The ethanol molecule which is H-bonded to the atom N4 of the benzimidazolate (O1E, C11E, C12E, figure 9) is disordered on two orientations with occupancies of 70 to 30 %. The other ethanol molecule (containing O2E) is disordered around a twofold axis, with an occupancy of 0.5 for all atoms. Thus, only half of these molecules are present simultaneously, whereas the other position remains unoccupied. This disorder results in an overall number of 3 ethanol molecules per perinone anion.
The ethanol molecules form layers parallel to the (100) direction, i.e., in the *bc*-plane (see figure 13 and figure 15). This ethanol layer contains short intermolecular C···C contacts of 2.5 to 3 Å. Such small distances are chemically unreasonable. They can only occur between the average atomic positions in in a highly dynamic structure or in disordered structure, in which not all atomic positions are occupied simultaneously. Most probably, both effects are present in **α-3**.

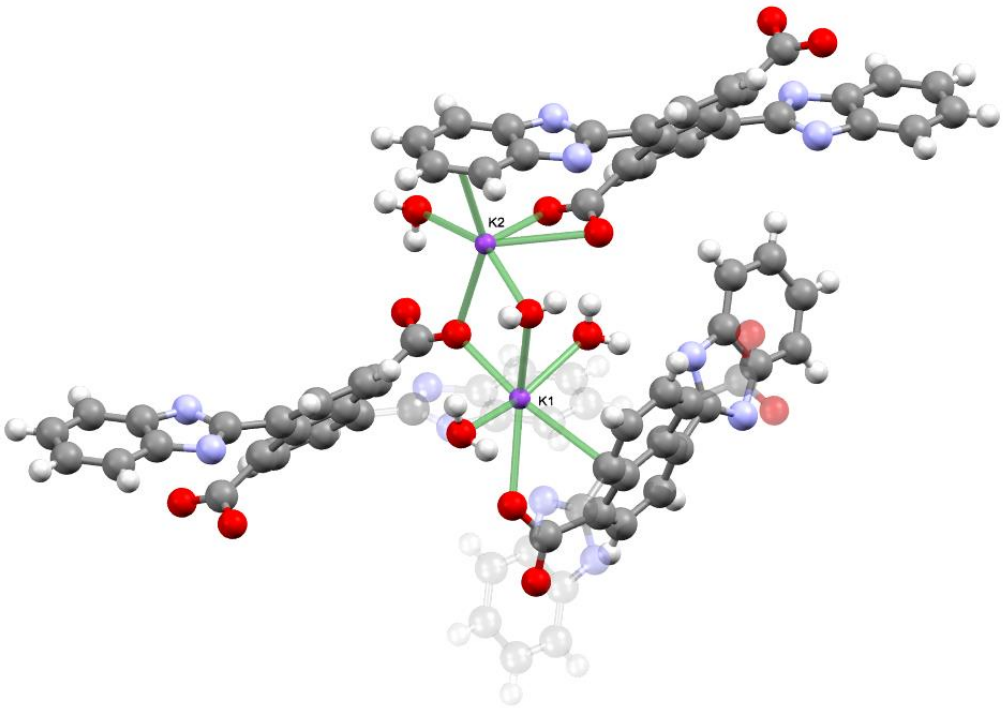

Figure 14: Coordinative environment of K1 (lower) and K2 (upper) in **α-3**. C atoms in grey, H white, O red, N blue, K violet. Coordinative bonds depicted as transparent green cylinders.

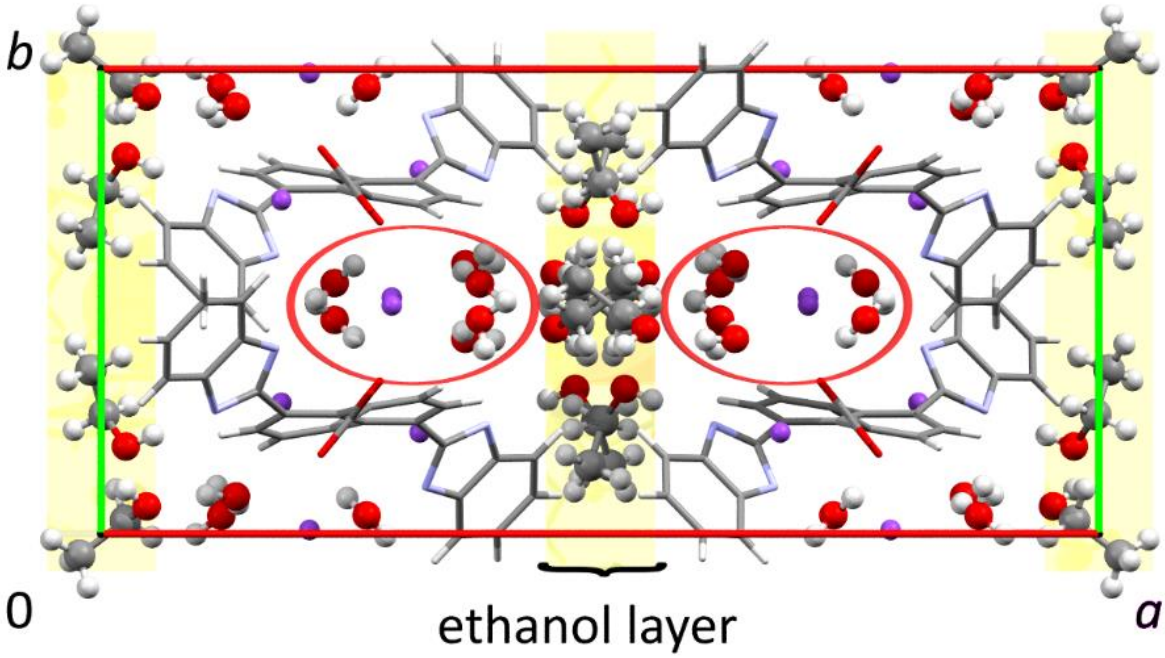

Figure 15: Crystal structure of **α-3**. View along the *c*-axis. The K_+ ions, ethanol and water molecules are drawn as ball-and-stick model, the tetra-anions as capped sticks only. The channels of water molecules are marked by a red ellipsis.

3.5.4 Dynamical aspects of the structure of α-3

The X-ray data reveal that both ethanol molecules in the structure **α-3** are disordered. The nature of the disorder, whether static or dynamic, was investigated by solid-state NMR spectroscopy. Depending on the type of experiment, solid-state NMR can either highlight signals arising from rigid or from highly dynamic parts of a structure. For rigid structures CPMAS (cross-polarization magic-angle spinning) experiments are employed. Dynamic, liquid-like aspects were investigated by MAS (direct excitation magic-angle spinning) experiments. [45,46] The ^{13}C CPMAS and MAS spectra of **α-3** are shown in figure 16.

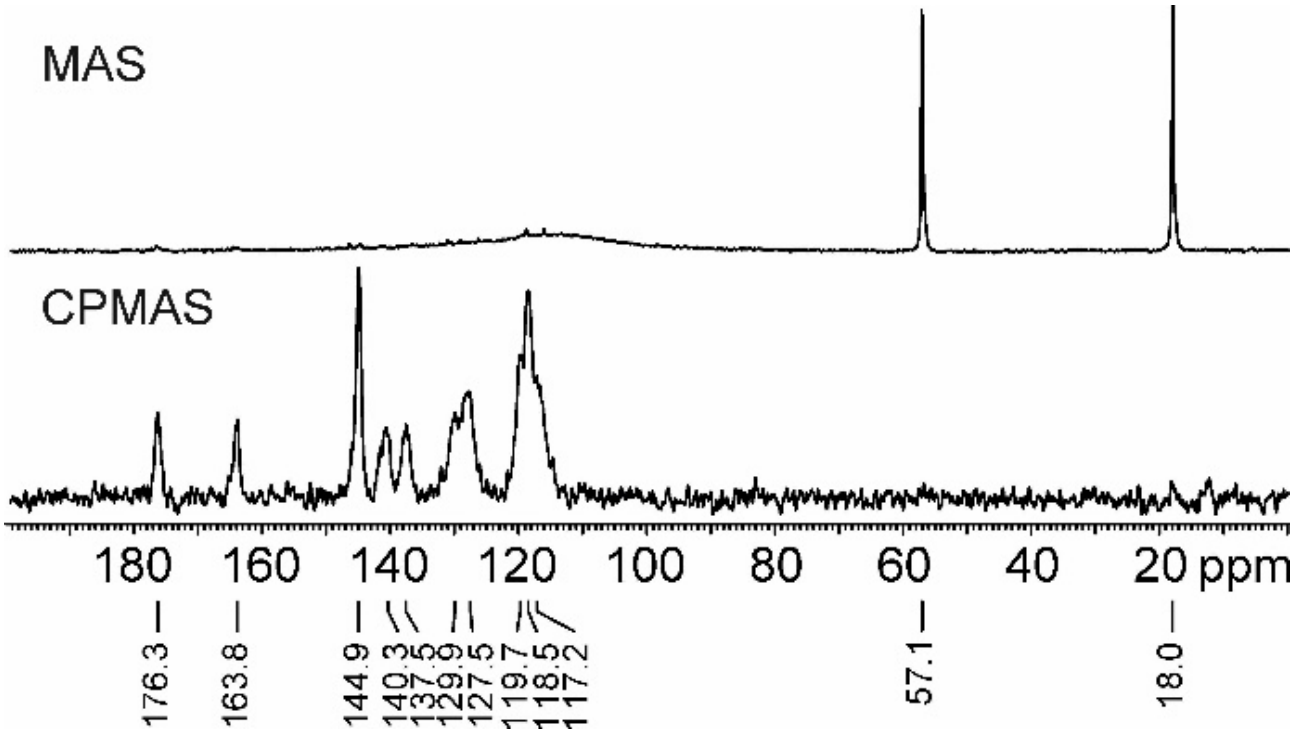

Figure 16: Solid-state NMR spectra of **α-3**. ^{13}C (150.9 MHz) CPMAS (bottom) and MAS (top) spectra acquired at a spinning speed of 20 kHz.

The 13C CPMAS spectrum shows aromatic and carbonyl resonances (around 110-150 and 160-180 ppm, respectively), which can be assigned to the rigid (in the NMR time scale) perinone tetra-anion. Interestingly, no aliphatic signals attributable to the ethanol molecules are present. Apparently, the ethanol is too dynamic to be seen in CPMAS spectra. On the other hand, the ^{13}C MAS spectrum is characterized by only two sharp peaks (~45 Hz width) at 18.0 and 57.1 ppm, which can be attributed to the ethanolic CH_3 and CH_2, respectively. Since the MAS experiments highlights resonances attributed to highly mobile moieties only, this clearly suggests a very fast exchange between all ethanol positions.
The crystal data show that such a fast exchange between all ethanol positions is well possible. All ethanol molecules are crystallographically disordered, leaving space at the respective momentarily unoccupied positions. There is enough space in the ethanol layer for the ethanol molecules to move from one position to another with only a small energy barrier. This fast movement explains the solution-like lines in the MAS spectrum.

3.5.5 Crystal structure of the β-phase of 3 (β-3)

Single-crystals of the β-phase of **3** (sample ***C***) could be obtained by recrystallization of sample ***A*** from a boiling mixture of KOH, water and ethanol (1:2:9). The crystal structure was determined from X-ray analysis.

The compound **β-3** crystallizes in the triclinic system with unit cell dimensions of a = 9.7342(9) Å, b = 16.3726(15) Å, c = 19.1558(17) Å, α = 9.7342(9)°, β = 84.851(7)° and γ = 77.963(7)°, resulting in a cell volume of 2784.0(5) $Å^3$ at 173(2) K. The space group is P 1.
Like **α-3**, also **β-3** contains a ring-opened tetra-anion. Even the conformation of the anion

is similar. The carboxylate groups as well as the benzimidazolate groups are rotated against the naphthalene plane[12], and bent out of the plane (figure 12).

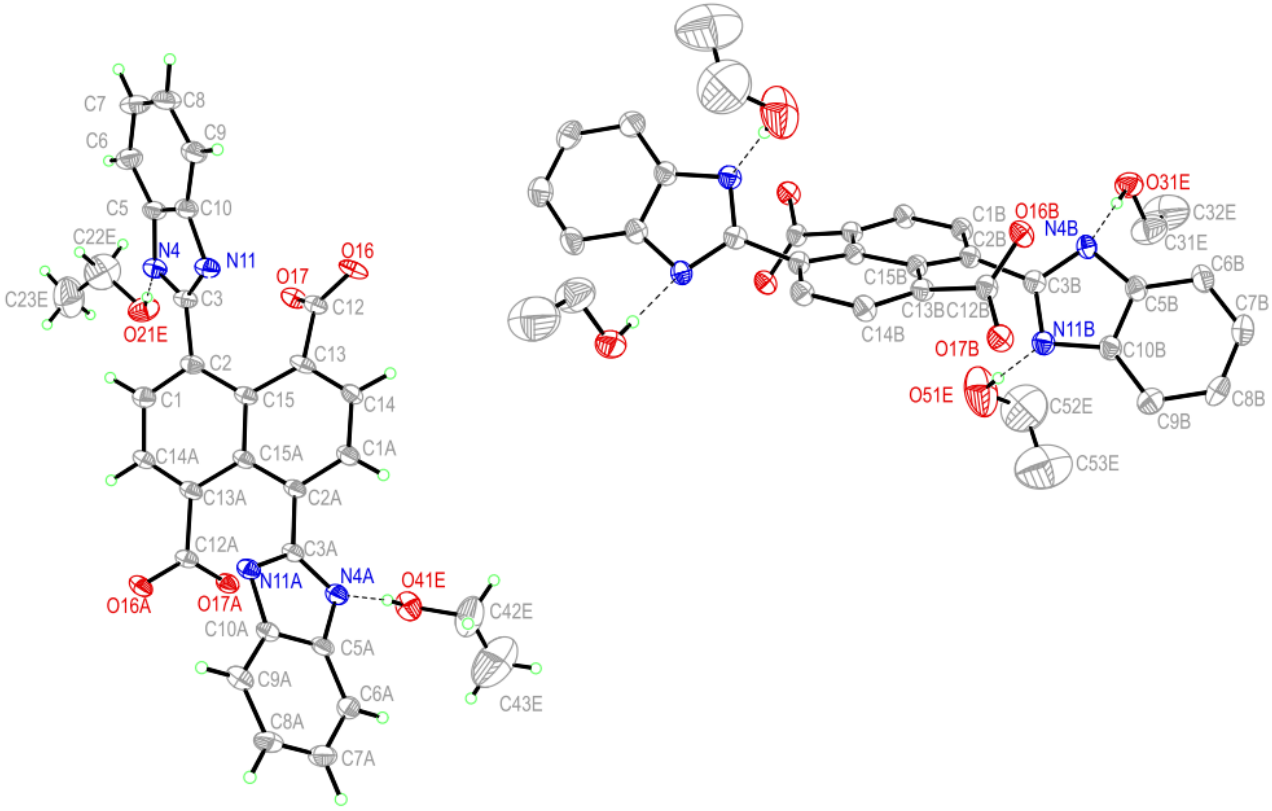

Figure 17: Ellipsoid plot (50 % probability) of **β-3**. Symmetry copies without label. One ethanol molecule and all water molecules and potassium ions omitted for clarity.
The unit cell contains three tetra-anions, with one of them on a crystallographic inversion centre and two on a general position.
The asymmetric unit is composed of one and a half perinone anions, six potassium cations, five molecules of ethanol and four water molecules. Correspondingly, the chemical composition of **β-3** is $1.5(K_4[C_{26}H_{12}N_4O_4])\cdot 5C_2H_5OH\cdot 4H_2O$.
All potassium ions, water and ethanol molecules are situated on a general position (see figure 18 and figure 19). The six unique potassium ions have coordination numbers of 6 to 8. The phase β-3 is a pseudopolymorph of α-3. Both phases contain the same tetra-

[12] Torsion angles for the COO group: φ(O16–C12–C13–C15) = -150.0(6)°, φ(O16A–C12A–C13A–C15A) = -132.6(6)°, φ(O16B–C12B–C13B–C15B) = 42.6(8)°; for the benzimidazole group: φ(N11–C3–C2–C15) = -37.8(9)°, φ(N11A–C3A–C2A–C15A) = 53.7(8) , φ(N11B–C3B–C2B–C15B) = 136.2(6).

anions, but differ in the numbers of ethanol and water molecules. In the α-phase there are 3 ethanol molecules and 6 water molecules per $K_4[C_{26}H_{12}N_4O_4]$ moiety. The β-phase contains 10/3 ethanol and 8/3 water molecules per $K_4[C_{26}H_{12}N_4O_4]$ moiety. The lower water content of the β-phase is in agreement with the higher temperatures during its crystallization, which generally hampers the inclusion of water molecules in the crystal lattice.

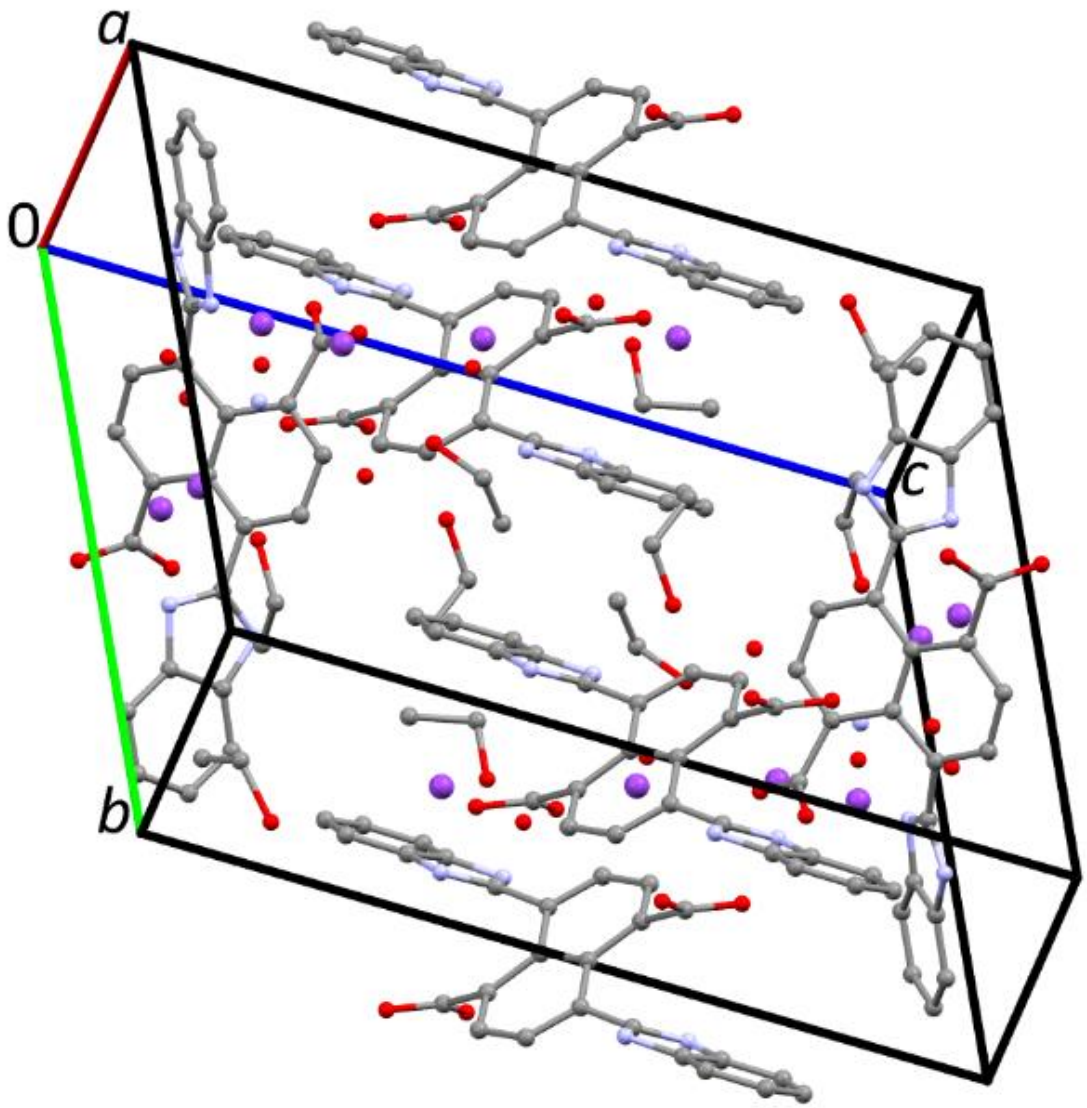

Figure 18: Crystal structure of **β-3**. H atoms are not shown.

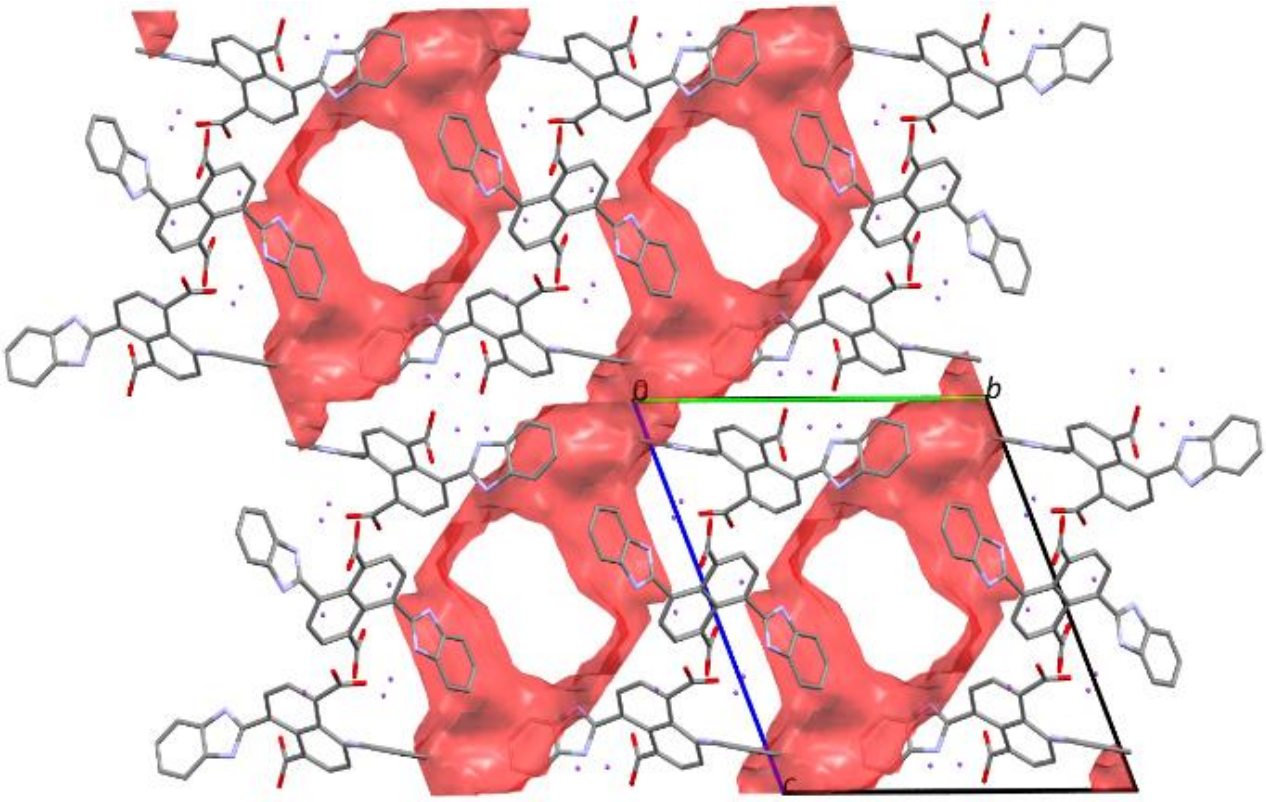

Figure 19: Crystal structure of **β-3**. Ethanol and water molecules are situated in channels. The outer surface of the channels is drawn in red. The channels are connected to a 2-dimensional layer formed by ethanol molecules. View along the *a*-axis.

In the crystal structure of **β-3**, the potassium cations and organic tetra-anions form a coordination network parallel to (011). The water and ethanol molecules are arranged in channels parallel to the *a*-axis, see figure 19. The channels are connected by close contacts between ethanol molecules[13], resulting in a layer of ethanol molecules parallel to (011), i.e. between the coordination network of K^+ cations and organic anions. Within these ethanol layers, the molecules are probably mobile and disordered, as it is evident from the large and anisotropic displacement parameters of the atoms of the ethanol molecules. However, the limited crystal quality of **β-3** does not allow detailed discussion of this disorder.

3.6 Crystal structure of the *cis*-intermediate (4)

Single-crystals of the *cis*-intermediate **4** have been obtained by reaction of pure **2** with KOH in ethanol and storage at elevated temperature (sample ***G***, see section 2.2). The crystal structure has successfully been determined at 293(2) K.

The intermediate **4** crystallizes in the monoclinic system in the space group $P\,2_1/n$. Crystallographic data are given in table 3.

The *cis*-intermediate **4** has a ring-opened structure, like the *trans*-intermediate **3**, see figure 20.

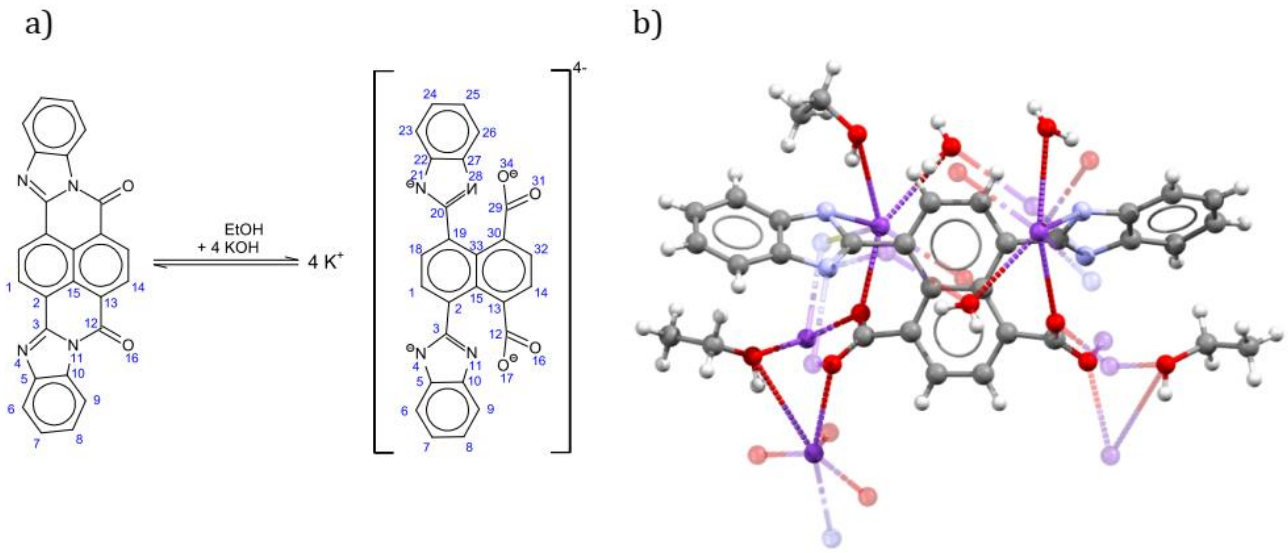

Figure 20: Structure of the *cis*-intermediate **4**. (a) Molecular structure. (b) Section from the crystal structure (coordinating symmetry copies depicted transparent).

The crystal quality was low, but better crystals could not be grown. Hence, the protonation state of the anion could not be determined from the X-ray data. In analogy to the investigations made on **α-3** and **β-3**, one should assume that the *cis*-intermediate, too, adopts the tetra-anionic state. Like in **α-3**, there is a hydrogen bond from the atom N4 of both benzimidazolate units to an ethanol molecule each (see figure 20b).

[13] d(C12E-C22E) = 3.727 Å.

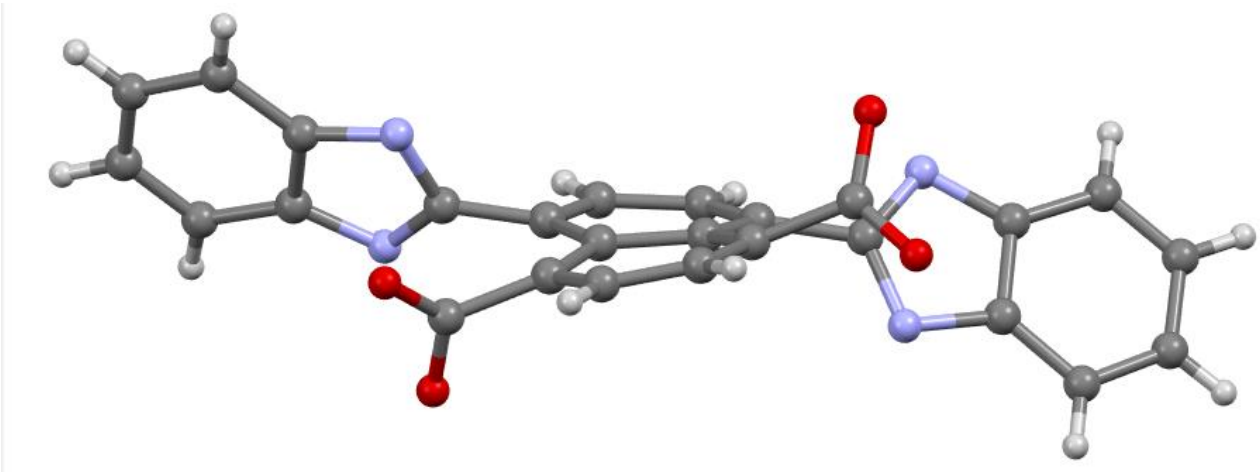

Figure 21: Organic anion in **4**.

The geometry of the *cis*-tetra-anion in the structure of **4** resembles the geometry of the *trans*-tetra-anions in the structures of **α-3** and **β-3**. Like in **3**, the carboxylate groups as well as the benzimidazolate groups are rotated against the naphthalene plane,[14] and bent out of the plane. This leads to a considerable distortion of the naphthalene plane, see figure 21.

The asymmetric unit is composed of one perinone tetra-anion, 4 potassium cations, 3 molecules of ethanol and 3 water molecules. Hence the chemical composition of **4** is:

$K_4[C_{26}H_{12}N_4O_4]\cdot 3C_2H_5OH\cdot 3H_2O$.
All four potassium cations coordinate directly to the N atoms of the benzimidazolate groups. This coordination is in contrast to **α-3**, where the benzimidazolate groups only act as π ligands to the K_+ ions. In **β-3**, both coordination modes are present.
The organic tetra-anions and potassium cations form a two-dimensional coordination network parallel to (010), i.e. parallel to the *ac*-plane, see figure 22.

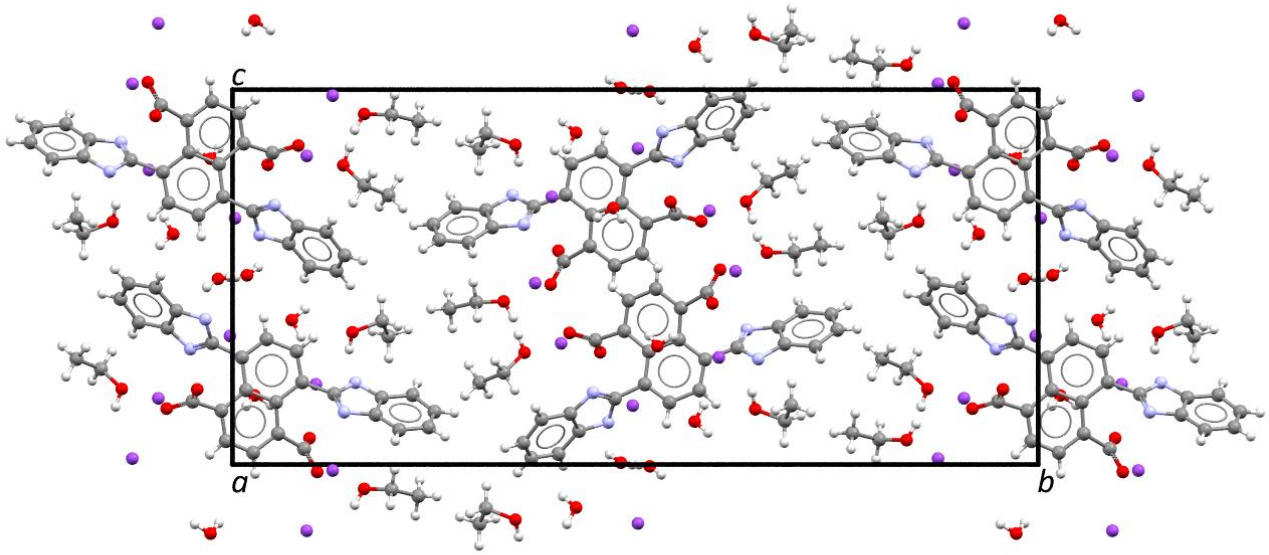

Figure 22: Crystal structure of the *cis*-intermediate **4**. View along the *a*-axis. C atoms in grey, H white, O red, N blue, K violet.

In KOH/ethanol solution, the ^{13}C NMR spectra of **4** show in total 10 signals, like for the *trans*-intermediate **3**. This proves, that the *cis*-intermediate **4** has a ring-opened structure in solution, like in the solid state. The protonation state of **4** in solution is not known, but presumably, the intermediate **4** is a tetra-anion like in the solid state. (See Fig. 19a)

3.7 On *leuco*-perinones (7, 8)

Upon reduction, the isomer mixture of perinones turns green, as described by Eckert & Greune in 1924 and 1926.[2,3] However, the molecular and crystal structure of resulting *leuco*-forms **7** (*trans*) and **8** (*cis*) are unknown till today. Reduction of the pure *trans*perinone **1** with potassium dithionite leads to a suspension of green colour. In the course
of our investigations, the *trans-leuco*-form **7** was isolated from this suspension by centrifugation, and analyzed. As a solid, **7** exhibits a dark green to black colour. All investigated samples of **7** were amorphous by means of X-ray diffraction.
No NMR-data of **7** could be obtained, because all isolated green solids (including **7**, prepared by reduction with dithionite) were insoluble in the usual solvents for NMR spectroscopy (including D_2O and ethanol-d_6).

A greenish substance of similar hue as **7** is obtained, when P.O.43 is stored in ethanolic KOH for three months at room temperature (720 mg **1**, 2 g KOH, 7.5 ml ethanol; sealed 10 ml flask). A powder X-ray diagram of this sample only showed reflections of poorly crystalline **3** (α-phase).
Samples of **3** in KOH/ethanol, stored at 50 °C for several weeks, produced a greenish solution and a slimy brown-reddish residue, which was amorphous by means of X-ray powder diffraction.
Hence, the molecular structure of the *trans-leuco*-form **7** and the chemical composition of the green suspension remain obscure.
The structure of the *cis-leuco*-form **8** was not investigated.

3.8 On the intermediates in the H_2SO_4 process

The dissolution of the perinone isomer mixture in concentrated sulfuric acid leads to a yellowish brown solution, as already observed by Eckert & Greune in 1924 [3]. From this solution, an "orange sulfate" (**5**) of the *trans*-isomer can be precipitated by cooling or by addition of a small amount of water.[3] According to our experiments, the solubility of perinone in sulfuric acid is quite high and moisture from air is sufficient to precipitate "orange sulfate" over the course of days. Without the addition of water, a considerable amount of perinone remains in solution at room temperature. The precipitate is rather complicated to isolate from the acid.
The orange sulfate can also be obtained by reaction of **1** with a vapour of sulfuric acid at 220 °C under reduced pressure.
Reaction of the obtained orange powders with water restores **1** and releases sulfuric acid.
The "orange sulfate" is more yellowish than **1** and the powder pattern of this (microcrystalline) substance strongly deviates from that of the starting material. The powder diagram indicates more than one phase; none of them could be identified (see ESI) and it was not possible to determine the crystal structure by powder diffraction, despite various attempts.
The ^{1}H and ^{13}C NMR data of a D_2SO_4 solution of **1** indicates, that the molecule retains its centrosymmetric structure (at least in time-average), and that no ring opening takes place (Sect. 3.2). The NMR data and the observed solubility can be explained by a protonated perinone molecule. However, the number of added protons and the protonation sites are not known.

Hence, the molecular structure of **5** and the chemical composition of the corresponding "orange sulfate" precipitate remain obscure.
The corresponding *cis*-intermediate **6** remains in solution in H_2SO_4, presumably as protonated species. Its ^{1}H and ^{13}C NMR spectra are similar to that of the *trans*intermediate **5**, but the signals are shifted. Further structural investigations have not been made.

4. Conclusion

After more than 80 years of industrial production, the molecular formulae of the intermediates in the industrial separation of perinone isomers are finally elucidated. Hitherto, neither their molecular structure, nor their crystal structures, nor even the chemical composition of the industrial precipitate of the *trans*-intermediate were known. In contrast to earlier assumptions, the intermediates **3** and **4** are no "KOH addition products", but products of a ring-opening reaction of the perinone skeleton (figure 23).

The distinction between the *cis*- and *trans*-isomers remains intact. The *trans*intermediate **3** has a lower solubility in KOH/ethanol, which allows the separation of the isomers. The ring-opening is reversible: Treatment of the isolated *trans*- and *cis*intermediates, **3** and **4**, with water leads to a ring-closure, restoring *trans*-perinone (**1**) and *cis*-perinone (**2**), respectively. Thus, the different solubilities of the intermediates **3** and **4** and the fully reversible ring openings allow the separation of the perinone isomers in the industrial process.

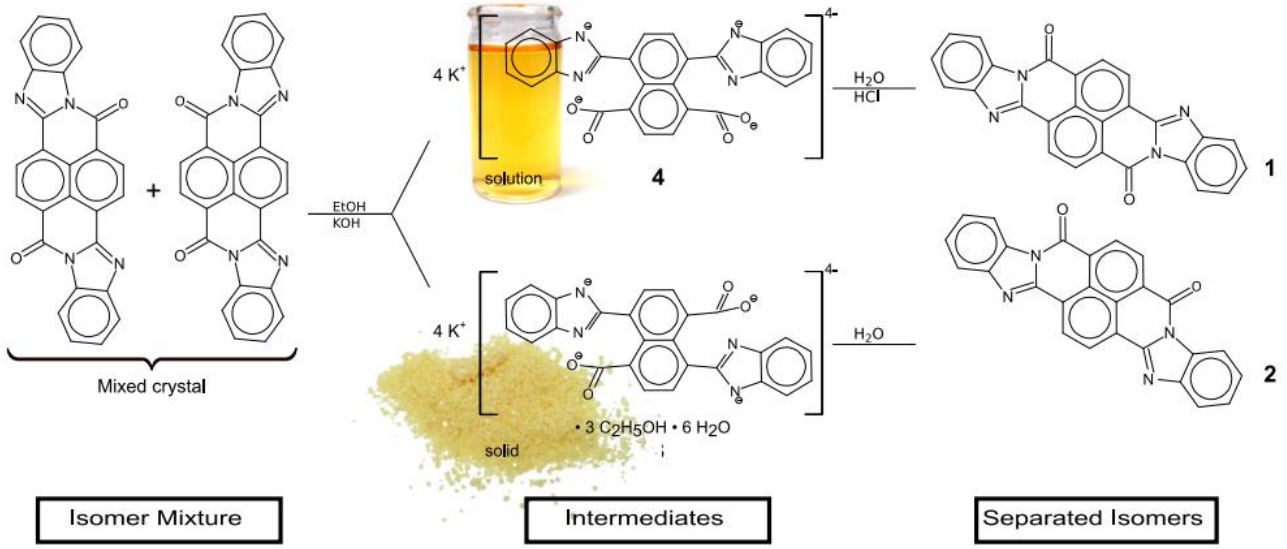

Figure 23: Structure of the intermediates in the industrial separation of perinone isomers.

In both perinone isomers, the ring-opening is accompanied by a rotation of the benzimidazolate moieties against the naphthalene fragment by 43° to 57.6°. This rotation results in an interruption of the conjugation of the π-systems, which causes the observed colour change from the bright orange *trans*-perinone (P.O.43, **1**) and the deep red *cis*perinone (P.R.194, **2**) to the almost colourless[15] intermediates **3** and **4**.

The *trans*-intermediate phase **α-3**, which precipitates from KOH/ethanol in the industrial process, contains ethanol and water molecules in its crystal lattice, and has a composition of $K_4[C_{26}H_{12}N_4O_4]\cdot 3C_2H_5OH\cdot 6H_2O$, as determined by single-crystal X-ray diffraction. A second crystal phase (**β-3**) of slightly different composition was synthesized and its structure was determined, too. The *cis*-intermediate (**4**), which is industrially handled only in solution, was isolated as a solid; a single crystal could be grown, and its structure was determined as well.

In the crystal structure of **α-3**, the potassium cations are π-coordinated to the benzimidazolate group, whereas they form a single coordination bond to the N atom of the benzimidazolate in **4**, and a mixture of both in **β-3**. In all structures, the water molecules are coordinated to the potassium cations, whereas the ethanol molecules occupy the voids between the molecules. The ethanol molecules form layers. According to solid-state NMR investigations of **α-3** (^{13}C CPMAS and MAS) the ethanol molecules are highly dynamic, whereas the organic anions are quite rigid.

The protonation state of the perinone anions could not be determined from single-crystal

data. NMR methods were used to identify the intermediate as tetra-anion and IR spectroscopy confirmed this conclusion. Besides the KOH/ethanol treatment, two other methods are known for the separation of the perinone isomers: fractionated crystallisation from sulfuric acid, or reduction to the *leuco* forms. The corresponding intermediates – protonated species or reduced species – were investigated, too, but their structures could not be unravelled, despite of various attempts.

Acknowledgements

The authors thank Sophie Müller (Clariant) for the industrial samples of perinone and of the intermediate **3**, Sibylle Aust (Clariant) for searches in the archives of Hoechst AG and Clariant, Christian Czech (Goethe University; now Amcapharm Pharmaceutical GmbH) for the support with CASTEP (DFT-D) calculations, Jan Klett (Johannes Gutenberg University, Mainz) for the Gaussian (*ab initio*) calculations, Yvonne Thiemann (Max Planck Institute of Biophysics, Frankfurt) for non-ambient X-ray experiments, Johanna Baldus and Clemens Glaubitz (both Goethe University) for preliminary solid-state NMR experiments, and Edith Alig (Goethe University) for the X-ray powder diffractograms.

15 The yellow colour of the precipitate **3** and of the solution of **4** in KOH/ethanol in the industrial process is apparently caused by impurities. The pure compounds **3** and **4** as crystalline solids are almost colourless.

References

[1] Eckert W, Sieber H. Verfahren zum Trennen von Küpenfarbstoffen. Deutsches Patent DE567210, 1932.
[2] Hunger K, Schmidt MU, Heber T, Reisinger F, Wannemacher S. Industrial Organic Pigments: Production, Crystal Structures, Properties, Applications, 4th, Completely Revised Edition. 4th ed. Weinheim: Wiley-VCH; 2018.
[3] Eckert W, Greune H. Verfahren zur Darstellung von Küpenfarbstoffen. DE430632, 1924.
[4] FIAT. German dyestuffs and dyestuff intermediates, including manufacturing processes, plant design, and research data / Field Information Agency Technical ; Vol. 1: Dyestuff intermediate processes and analytical procedures. Washington, DC: Office of Military Government for Germany (U.S.); 1948.
[5] Fierz-David HE, Rossi C. Über die Darstellung von Naphthoylen-imidazolinen. Helv Chim Acta 1938;21:1466–89. https://doi.org/10.1002/hlca.193802101182.
[6] Teteruk JL, Glinnemann J, Heyse W, Johansson KE, van de Streek J, Schmidt MU. Local structure in the disordered solid solution of *cis* - and *trans* -perinones. Acta

Crystallogr	Sect	B	Str uct	Sci	Cry st	Eng	Mat er	2016;72: 416–33.
https://doi.org/10.1107/S205 2520616004972.								
[7] Mizuguchi J. Crystal Structure and Electronic Characterization of *trans* - and *cis* -								
Perinone	Pigme nts.	J	Phy s	Che m	B	2004;108: 8926–30.		

https://doi.org/10.1021/jp031351d.
[8] Paulus EF, Kunstmann W. Forschungsbericht 265 III.3. Hoechst Am Main: Hoechst

AG; 1978.
[9] Mizuguchi J. Crystal structure of trans-bisbenzimidazo[2,1-b:1',2'-j]benzo[lmn][3,8]-phenanthroline-6,9-dione, C26H12N4O2. Z Für Krist - New Cryst Struct 2003;218. https://doi.org/10.1524/ncrs.2003.218.1.137.
[10] Mizuguchi J. Crystal structure of bisbenzimidazo[2,1-b:2',1'-i]benzo[lmn][3,8]phenanthroline- 8,17-dione, C26H12N4O2. Z Für Krist - New Cryst Struct 2003;218. https://doi.org/10.1524/ncrs.2003.218.1.139.
[11] Zherebtsov DA, Schmidt MU, Niewa R, Sakthidharan CP, Podgornov FV, Matveychuk YV, et al. Two new polymorphs of *cis* -perinone: crystal structures, physical and electric properties. Acta Crystallogr Sect B Struct Sci Cryst Eng Mater 2019;75:384–92. https://doi.org/10.1107/S2052520619003287.
[12] Herbst W, Hunger K, Wilker G. Industrial organic pigments: production, properties, applications. 3rd ed. Weinheim: Wiley-VCH; 2004.
[13] Clariant. internal document on the synthesis of P.O.43, 2008.
[14] Fierz-David HE, Rossi C. Über die Darstellung von Naphthoylen-imidazolinen. Helv Chim Acta 1938;21:1466–89. https://doi.org/10.1002/hlca.193802101182.
[15] Schultz G. Farbstofftabellen. Band 1: Künstliche organische Farbstoffe bekannter Konstitution oder Herstellungsweise. vol. 1. Leipzig: Akademische Verlagsgesellschaft; 1931.
[16] Eckert W. Verfahren zur Darstellung von Küpenfarbstoffen. DRP456236, 1928.
[17] Eckert W, Greune H. Verfahren zur Darstellung von Küpenfarbstoffen. DRP457980, 1928.

[18] Neresheimer H, Eichholz W. Verfahren zur Darstellung von orange färbenden Küpenfarbstoffen. DRP507832, 1940.
[19] A. Schaeffer. Die Küpenfarbstoffe. Aufbau, Eigenschaften, Anwendung. Band A: Aufbau der Küpenfarbstoffe. vol. A. Hoechst Am Main: Farbwerke Hoechst; 1948.
[20] Die Küpenfarbstoffe und ihre Verwendung in der Färberei und im Zeugdruck. Vienna: Springer Vienna; 1953.
[21] Dietz E, Kapaun G, Schiessler S. Verfahren zur Herstellung von Küpenfarbstoffen und Pigmenten der Perinon-Reihe. Deutsches Patent DE3836674A1, 1990.
[22] Taublaender MJ, Glöcklhofer F, Marchetti-Deschmann M, Unterlass MM. Green and Rapid Hydrothermal Crystallization and Synthesis of Fully Conjugated Aromatic Compounds. Angew Chem Int Ed 2018;57:12270–4. https://doi.org/10.1002/anie.201801277.
[23] European Parliament. Commission Regulation (EC) No 1223/2009 of the European Parliament and of the Council of 30 November 2009 on cosmetic products; Official Journal of the European Union. 2009.
[24] Imperial Leather UK. Product Packaging "Imperial Leather soap classic packaging"; Ingredients declaration 2018.
[25] Intoglam corp. Material Safety Data Sheet: Color Gel by Intoglam. 2016.
[26] Piccinini P, Contor L, Pakalin S, Senaldi C, Raemaekers T, Institute for Health and Consumer Protection. Safety of tattoos and permanent make-up: state of play and trends in tattoo practices. Luxembourg: Publications Office; 2015.
[27] Holleman AF, Wiberg N. Lehrbuch der anorganischen Chemie. 102., stark umgearbeitete und verbesserte Auflage. Berlin New York: Walter de Gruyter; 2007.
[28] Taublaender MJ, Glöcklhofer F, Marchetti-Deschmann M, Unterlass MM. Green and

Rapid Hydrothermal Crystallization and Synthesis of Fully Conjugated Aromatic Compounds. Angew Chem Int Ed 2018;57:12270–4. https://doi.org/10.1002/anie.201801277.
[29] David WIF, Shankland K, van de Streek J, Pidcock E, Motherwell WDS, Cole JC. DASH: a program for crystal structure determination from powder diffraction data. J Appl Crystallogr 2006;39:910–5. https://doi.org/10.1107/S0021889806042117.
[30] STOE & Cie GmbH. www.stoe.com n.d.
[31] Sheldrick GM. A short history of *SHELX*. Acta Crystallogr A 2008;64:112–22. https://doi.org/10.1107/S0108767307043930.
[32] Sheldrick GM. SADABS. Karlsruhe, Germany: Bruker AXS; 1996.
[33] Clark SJ, Segall MD, Pickard CJ, Hasnip PJ, Probert MIJ, Refson K, et al. First principles methods using CASTEP. Z Krist – Cryst Mater 2005;220. https://doi.org/10.1524/zkri.220.5.567.65075.
[34] Vanderbilt null. Soft self-consistent pseudopotentials in a generalized eigenvalue formalism. Phys Rev B Condens Matter 1990;41:7892–5.
[35] Perdew JP, Burke K, Ernzerhof M. Generalized Gradient Approximation Made Simple. Phys Rev Lett 1996;77:3865–8. https://doi.org/10.1103/PhysRevLett.77.3865.
[36] Grimme S. Semiempirical GGA-type density functional constructed with a long-range dispersion correction. J Comput Chem 2006;27:1787–99. https://doi.org/10.1002/jcc.20495.
[37] Mayo SL, Olafson BD, Goddard WA. DREIDING: a generic force field for molecular simulations. J Phys Chem 1990;94:8897–909. https://doi.org/10.1021/j100389a010.
[38] Frisch MJ, Trucks GW, Schlegel HB, Scuseria GE, Robb MA, Cheeseman JR, et al. Gaussian 09, Revision B.01. Wallingford CT: Gaussian, Inc.; 2009.

[39] Batamack P, Fraissard J. Proton NMR studies on concentrated aqueous sulfuric acid solutions and Nafion-H. Catal Lett 1997;49:129–136.
[40] Markvardsen AJ, David WIF, Johnston JC, Johnson JC, Shankland K. A probabilistic approach to space-group determination from powder diffraction data. Acta Crystallogr A 2001;57:47–54.
[41] Pawley GS. Unit-cell refinement from powder diffraction scans. J Appl Crystallogr 1981;14:357–61. https://doi.org/10.1107/S0021889881009618.
[42] Bruno IJ, Cole JC, Kessler M, Luo J, Motherwell WDS, Purkis LH, et al. Retrieval of Crystallographically-Derived Molecular Geometry Information. J Chem Inf Comput Sci 2004;44:2133–44. https://doi.org/10.1021/ci049780b.
[43] Etter MC, MacDonald JC, Bernstein J. Graph-set analysis of hydrogen-bond patterns in organic crystals. Acta Crystallogr B 1990;46:256–62. https://doi.org/10.1107/S0108768189012929.
[44] Grell J, Bernstein J, Tinhofer G. Graph-set analysis of hydrogen-bond patterns: some mathematical concepts. Acta Crystallogr B 1999;55:1030–43. https://doi.org/10.1107/S0108768199007120.
[45] Chierotti MR, Amin M, Hassan YS, Haikal RR, Garino C, Alkordi MH. Combined SolidState NMR and Computational Approach for Probing the CO 2 Binding Sites in a Porous-Organic Polymer. J Phys Chem C 2017;121:8850–6. https://doi.org/10.1021/acs.jpcc.7b00660.
[46] d'Agostino S, Fornasari L, Grepioni F, Braga D, Rossi F, Chierotti MR, et al.

Precessional Motion in Crystalline Solid Solutions of Ionic Rotors. Chem - Eur J 2018. https://doi.org/10.1002/chem.201803071.